ISTANBUL TECHNICAL UNIVERSITY ★ GRADUATE SCHOOL OF SCIENCE ENGINEERING AND TECHNOLOGY

DESIGN AND CHARACTERIZATION OF NOVEL O/W/O DOUBLE EMULSIONS

M.Sc. THESIS

Turgay ÇETİNKAYA

Department of Food Engineering

Food Engineering Program

JUNE 2016

ISTANBUL TECHNICAL UNIVERSITY ★ GRADUATE SCHOOL OF SCIENCE ENGINEERING AND TECHNOLOGY

DESIGN AND CHARACTERIZATION OF NOVEL O/W/O DOUBLE EMULSIONS

M.Sc. THESIS

Turgay ÇETİNKAYA
(506141534)

Department of Food Engineering

Food Program Engineering

Thesis Advisor: Assoc. Prof. Dr. Filiz ALTAY

JUNE 2016

İSTANBUL TEKNİK ÜNİVERSİTESİ ★ FEN BİLİMLERİ ENSTİTÜSÜ

YENİ NESİL Y/S/Y ÇİFT KATLI EMÜLSİYONLARININ TASARIMI VE KARAKTERİZASYONU

YÜKSEK LİSANS TEZİ

Turgay ÇETİNKAYA
(506141534)

Gıda Mühendisliği Anabilim Dalı

Gıda Mühendisliği Programı

Tez Danışmanı: Doç. Dr. Filiz ALTAY

HAZİRAN 2016

Turgay ÇETİNKAYA, a M.Sc. student of ITU Graduate School of Science Engineering and Technology student ID 506141534, successfully defended the thesis/dissertation entitled "DESIGN AND CHARACTERIZATION OF NOVEL O/W/O DOUBLE EMULSIONS", which he prepared after fulfilling the requirements specified in the associated legislations, before the jury whose signatures are below.

Thesis Advisor :	**Assoc. Prof. Dr. Filiz ALTAY** Istanbul Technical University	.....
Jury Members :	**Ass. Prof. Dr. Funda Karbancıoğlu GÜLER** Istanbul Technical University	.....
	Ass. Prof. Dr. Zeki DURAK Yıldız Technical University	.....

Date of Submission : 02 May 2016
Date of Defense : 10 June 2016

To my family,

FOREWORD

I would like to express my sincere gratitude to my supervisor, Assoc. Prof. Dr. Ashok PATEL for his support for my master thesis research and study. I am thankful to Prof. Patel for providing me with an opportunity to work in Vandemoortele Lipid Centre as an Erasmus student in collaboration with the laboratory of Food Technology and Engineering, Ghent University, Belgium.

I also sincerely thank my sister Miss Thin Amy CHIT, my mentor Mohd Dona bin SINNTAG, Phd. students Viet, Mathias, Wahyu and other laboratory staffs for their support, advice and guidence during the time period of my thesis work.

Finally I would like to express my sincerest appreciation and profound gratitude to my thesis advisor Assoc. Prof. Dr. Filiz ALTAY for her support and assistance during my thesis writing stage at Istanbul Technical University, Turkey.

May 2016

Turgay ÇETİNKAYA
(Food Engineer)

TABLE OF CONTENTS

Page

ABBREVIATIONS

O/W	**:** Oil-in-water
W/O	**:** Water-in-oil
O/W/O	**:** Oil-in-water-in-oil
W/O/W	**:** Water-in-oil-in-water
Wt	**:** Weight
PE	**:** Primary Emulsion
DE	**:** Double Emulsion
GL	**:** Gelatin
XG	**:** Xanthan gum
SFO	**:** Sunflower oil
Rpm	**:** Rotation per minute
PLM	**:** Polarized light microscopy
LVR	**:** Linear viscoelastic region
HLB	**:** Hydrophilic-lipophilic balance
DSD	**:** Droplet size distribution
PGPR	**:** Polyglycerol-polyricinoleate
Pfg-NMR	**:** Pulsed field gradient nuclear magnetic resonance
Cryo-SEM	**:** Cryogenic scanning electron microscopy
DSC	**:** Differential scanning calorimetry
Tween 80	**:** Polyoxyethylene-20 sorbitan monooleate
Span 80	**:** Sorbitane monooleate
PEG 300	**:** Polyethylene Glycol 300
SD	**:** Standart deviation

SYMBOLS

Hz	**:** Hertz
G'	**:** Storage modulus
G''	: Loss modulus
R_{43}	**:** Arithmetic mean droplet radius
σ	**:** Arithmetic standard deviation
Δ	**:** Diffusion time
N	**:** Newton
µm	**:** Micrometer
nm	**:** Nanometer
T_0	**:** Peak starting temperature
T_p	**:** Peak temperature
T_e	**:** Peak end temperature
ΔH	**:** Heat energy

LIST OF TABLES

Page

LIST OF FIGURES

Page

DESIGN AND CHARACTERIZATION OF NOVEL OIL-IN-WATER-IN-OIL DOUBLE EMULSIONS

SUMMARY

In this study oil-in-water-in-oil (O/W/O) systems which can be called double emulsion (DE) were formulated by using biopolymers. To formulate DE, first oil was dispersed in water. This process is referred oil-in-water O/W emulsion, then this emulsion was dispersed in a second oil phase. As they are more complicated to produce and more susceptible to breakdown there are only a few published researches about O/W/O systems. In this research O/W/O DEs were designed by fat crystallization method in a two stage emulsification method; in the first step primary emulsion (PE) was formulated which stabilized with biopolymers, and in the second step hardstock was added to the PE to get a structured oil system. Consequently, biopolymers were used to stabilize oil-in-water (O/W) emulsions and these emulsions were used further as template to generate the O/W/O emulsion with low solid fat content. Specific objectives were; to formulate O/W/O DEs at different proportion of liquid oil, hardstock, water and to characterize them in terms of microscopic structure, droplet size distribution, rheology, texture and thermal stability. A new approach was investigated that use of less solid fat in converting liquid oil into internal water droplets to get similar structure. Initially, sunflower oil (SFO) was dispersed in stock solutions containing gelatin (GL) at 10 weight% (wt) and xanthan gum (XG) at 2 wt% to develop PE. Three PEs at the oil/water ratio of 6:4 (I), 2:8 (II) and 1:9 (III) were prepared by using a high-energy dispersing unit Ultraturrax. For the DE preperation step, O/W ratio of 6:4 (I) emulsion was used in the first process. Varying amounts of palm oil (melted at 50 ˚C) and SFO added to 6:4 PE (I) then mixture homogenized with Ultraturrax. Emulsions containing SFO at 30 wt% (IV), 38.3 wt% (V), 46.7 wt% (VI) and 55 wt% (VII) were obtained while cooling them at -0.15 ˚C after two minutes of homogenization. In this way, fat crystallization occured and DE formation was observed. For next process, DEs prepared from 2:8 O/W ratio of (II) PE. Different amount of palm oils was directly added to PEs and mixture was subjected to cooling at -0.15 ˚C during homogenizing. As a result, DEs at 30 wt% (VIII), 40wt% (IX) and 45 wt% (X) water were obtained just by using natural emulsifier (GL) and stabilizer (XG). For achieving DE at 60 wt% (XI) water a lipophilic surface active agent polyglycerol-polyricinoleate was used at 0.4 wt%. For the last process 6:4 O/W ratio of PE (I) was used but water concentration varied at 20 wt% (XII) and 26.67 wt% (XIII).

The microstructures of these systems were recorded by optical microscopy and cryogenic scanning electron microscopy. Microscopic images revealed the morphology of emulsions. Oil droplets and internal water droplets in emulsions can clearly be seen under polarized light and normal light. The light scattering method by Mastersizer was used to determine the average volume weighted droplet size of PEs. Droplet sizes measured as 9.22 ± 2.29 μm (I), 17.21 ± 1.05 μm (II), 16.89 ± 0.63 μm

(III) respectively. Pulsed field gradient nuclear magnetic resonance (Pfg-NMR) was used to measure water droplet size of DEs. Droplet sizes measured as 8.91 ± 0.51 μm (Δ=36 second) and 10.23 ± 0.07 μm (Δ=66 second). The effect of different SFO concentrations (at 20 wt% water) and different water concentrations (at 20%, 26.67 wt%, 30 wt%, 40 wt%, 45 wt%, 60 wt% water) on the rheological and textural characteristics of emulsions were also evaluated using rheometer and texture analyzer to understand these systems. Texture analyses confirmed that hardness values decreased proportionally to the increasing SFO content from 30 wt% to 55 wt% at constant water ratio. Hardness values measured as 13.40 ± 1.68 N (IV), 9.70 ± 2.13 N (V), 8.12 ± 0.70 N (VI), 3.42 ± 0.61 N (VII) respectively. By increasing water content from 20 wt% to 60%, hardness values were also decreased. At different water concentrations hardness values were 58.99 ± 6.45 N (VIII), 27.47 ± 4.43 N (IX), 39.04 ± 2.13 N (X), 6.32 ± 0.67 N (XI). However, hardness values did not show major difference at 20 wt% and 26.67 wt% water. Amplitude sweep stress and frequency sweep tests were applied to understand viscoelastic behavior of emulsions. DEs showed weak gel structure and elastic behavior. Gel stiffness decreased by increasing water ratio which means that rheological results were in agreement with the results from texture analysis. Differential Scanning Calorimetry (DSC) was used to determine peak temperatures and heat absorption (melting) of samples. Thermograms confirmed that palm oil solidified during DE formation. DE samples stored in certain periods at 4 ˚C and recorded by optical microscopy. DE structure was still provided but water phase started to broke and emulsion stability decreased.

The results of this work showed that the encapsulation of SFO by using GL and XG could be significant for producing reduced-fat products. Additionally, the optimization and the formulation of DEs with this method could be further used as a template for the encapsulation of flavors or other components.

YENİ NESİL Y/S/Y ÇİFT KATLI EMÜLSİYONLARININ TASARIMI VE KARAKTERİZASYONU

ÖZET

Bu çalışmada yağ içinde su içinde yağ (Y/S/Y) sistemleri biyopolimerler kullanılarak formüle edilmiştir. Bu sistemlere çift katlı emülsiyonlar veya çoklu emülsiyonlar diyebiliriz. Çoklu emülsiyonlar yağ içinde su (Y/S) ve su içinde yağ (S/Y) emülsiyon yapılarının her ikisini de içerirler ve yağ içinde su içinde yağ (Y/S/Y) veya su içinde yağ içinde su (S/Y/S) olmak üzere iki ana yapıda olurlar. Y/S/Y çoklu emülsiyonların formülasyonunda öncelikle yağ, su içinde çözündürülür. Bu yapı birincil emülsiyon olarak adlandırılır. Daha sonra emülsiyon ikinci bir yağ fazı içinde tekrar çözündürülür. Çalışmada emülsiyonlar yağ kristalizasyonu prensibine dayanan iki aşamalı emülsifikasyon yöntemiyle hazırlanmıştır. Birincil Y/S emülsiyonu doğal biyopolimerlerle stabilize edilip tasarlanmıştır ve daha sonra bu emülsiyona palm yağı eklenerek düşük katı yağ içeren Y/S/Y sistemleri oluşturulmuştur. Böylece ayçiçek yağının su damlacıklarının içine aktarılmasıyla ilgili yeni bir yaklaşım incelenmiştir. Çalışmanın özel hedefleri Y/S/Y çift katlı emülsiyonlarını farklı sıvı yağ, katı yağ ve su oranlarında tasarlamak ve bu emülsiyonları mikroskobik yapı, partikül boyut dağılımı, reoloji, tekstür ve termal stabilite özellikleri açısından karakterize etmektir. Birincil emülsiyonun bileşenleri için jelatin, ksantan gam ve ayçiçek yağı kullanılmıştır. Jelatin ve ksantan gam stok çözeltileri belirli miktarlarda polimer tozlarının arıtılmış suya eklenmesiyle hazırlanmıştır. Jelatin tozları beherde %10'luk solüsyon olacak şekilde tartılmıştır. Daha sonra çözelti manyetik karıştırıcıda 50 ˚C'de 30 dakika boyunca karıştırılmıştır. Ksantam gam tozlarından ise %2'lik solusyon hazırlanmış ve arıtılmış suda tamamen çözülene kadar manyetik karıştırıcıda karışması sağlanmıştır. Ayçiçek yağı kullanılmadan önce 4 ˚C'lik buzdolabında bekletilmiştir.

Birincil emülsiyon için 6:4 (I), 2:8 (II), 1:9 (III) oranlarında üç farklı Y/S karışımı hazırlanmıştır. 6:4 oranındaki emülsiyon için 36 gram ayçiçek yağı, 12 gram ksantan gam ve 6 gram jelatin; 2:8 oranındaki emülsiyon için 12 gram ayçiçek yağı, 42 gram ksantan gam, 6 gram jelatin; 1:9 oranındaki emülsiyon için 6 gram ayçiçek yağı, 48 gram ksantan gam ve 6 gram jelatin kullanılmıştır. Öncelikle kapların içerisine terazi üzerinde tartılan miktarlarda polimerlerden ve ayçiçek yağından aktarılmıştır. Daha sonra karışım yüksek enerjili parçalama ünitesinde homojenize edilmiştir. Ürünlerden küçük bir damla örnek alınıp lam üzerine yerleştirilmiştir ve lamel ile hafifçe bastırılarak örnek yayılmıştır. Daha sonra optik mikroskop altında incelenmiştir. Bir protein olan jelatin hem hidrofil hem de hidrofob parçalara sahip olup doğal emülgatör görevi gördüğünden, ksantan gam ise emülgatör özelliği olmasa da iyi bir stabilizör olduğundan iki polimerin birlikte kullanılmasıyla Y/S emülsiyonunun yapısının belirdiği ve ayçiçek yağı damlacıklarının etrafında polimer ağının oluştuğu örnekler mikroskopta incelendiğinde net bir şekilde görülmüştür. Daha sonra ikinci aşama olan çift katlı emülsiyonların hazırlanmasına geçilmiştir.

Çift katlı emülsiyonlar üç farklı şekilde hazırlanmıştır. İlk önce 6:4 (I) oranındaki Y/S emülsiyonu kullanılmıştır. 50 ˚C'de etüvde eritilen palm yağı değişen miktarlarda ayçiçek yağıyla karıştırılmış ve daha sonra karışıma birincil emülsiyon eklenmiştir. Sırasıyla %30 (IV), %38,3 (V), %46,7 (VI) ve %55 (VII) ağırlıklarında ayçiçek yağı içeren karışımlar homojenize edilerek çift katlı emülsiyonlar elde edilmiştir. Sonuç olarak son üründe su oranı %20'de sabit tutularak palm yağı oranının düşürülmesi amaçlanmıştır. Emülsiyonlar hazırlanırken Ultraturrax T 25B markalı homojenizatörde karıştırılmıştır. İkinci ve üçüncü tipteki çift katlı emülsiyonların hazırlanması için ise Ultraturrax-T 25 Dijital S25KV markalı homojenizatör kullanılmıştır. İkinci tipteki emülsiyonlar 2:8 (II) oranındaki Y/S emülsiyonun değişik miktarlarda kullanılmasıyla oluşturulmuştur. Böylece su oranı %30 (VIII), %40 (IX), %45 (X), ve %60 (XI) olacak şekilde ayarlanmıştır. İlk prosesten farklı olarak palm yağı doğrudan Y/S emülsiyonuna eklenmiştir. Çalışmalarda %30, %40 ve %45 su içeriğine kadar herhangi bir sentetik yüzey aktif madde kullanmadan çift katlı emülsiyonlar başarıyla elde edilmiştir. Sadece %60 oranında su içeren Y/S/Y emülsiyonunu elde edebilmek için lipofilik yüzey aktif madde olan poligliserol-polirikinoleat %0,4 oranında kullanılmıştır. Üçüncü tipteki emülsiyonlarda ise yine 6:4 oranında Y/S emülsiyonu kullanılmış ancak su oranı %20 (XII) ve %26,67 (XIII) olacak şekilde ayarlanmıştır. Y/S/Y emülsiyonları hazırlanırken tüm işlemlerde homojenizasyon esnasında palm yağının kristalleşerek katılaşması ve emulsiyonun stabil hale geçmesi için ikinci dakikadan itibaren kapların altına buzlu su yerleştirilmiştir. Karışımlar -0,15 ˚C'ye kadar soğutulmuştur ve ayçiçek yağının su fazında hapsedilmesi sağlanmıştır. Su oranına göre değişmekle birlikte toplam homojenizasyon süresi 9 ile 18 dakika arasında ayarlanmıştır. Palm yağının katılaşarak kristalleşmesi küre şekillerinde küçük su fazlarının oluşmasını sağlamıştır. Böylece karışımın stabilize olarak Y/S/Y çift katlı emülsiyon yapısına dönüşümü gerçekleşmiştir. Örnekleri incelemek için küçük bir miktarda alınıp lam üzerine yerleştirilmiştir ve lamel ile hafif bastırılıp yayılmıştır. Su fazı içine transfer olmuş yağ damlacıklarının polarize ve normal ışık altında fotoğrafları çekilerek optik mikroskop ile incelenmiştir. Mikroskobik resimler yağ damlacıklarını, su fazını ve polarize ışık altında mavi renk veren dış fazdaki palm yağı kristallerini net bir şekilde görmemize yardımcı olarak emülsiyonların morfolojisini ortaya çıkarmıştır. Y/S ve Y/S/Y sistemlerinin mikroyapıları krayojenik tarama elektron mikroskobu kullanılarak da incelenmiştir. Su fazının tamamen uzaklaştırılması prensibine dayanan yöntemde birincil emülsiyonda polimerlerin yağ ara yüzeyinde ve dış fazda belirgin bir ağ oluşturduğu gözlemlenmiştir. Polimerlerin (jelatin ve ksantan gam) yağ damlacıklarının etrafındaki varlığı yağ damlacıklarının birleşmesini önlediğini göstermiştir. Y/S emülsiyonlarında ortalama partikül boyutu hakkında bilgi sahibi olmak için ışığın saçılması prensibine dayanan parçacık büyüklüğü analiz cihazı kullanılmıştır. Örneklerden 1'er gram alınarak 100 gram arıtılmış su içerisinde çözülmüştür. Seyreltilen örneklerin damlacık boyutu sırasıyla 9,22 ± 2,29 μm (I), 17,21 ± 1,05 μm (II), 16,89 ± 0,63 μm (III) ölçülmüştür. Sonuçlar sabit jelatin oranında ksantan gam oranı artığında emülsiyonların ortalama partikül boyutunun büyüdüğünü göstermiştir. Nükleer manyetik rezonans spektroskopisi, 30/20/50 (IV) çift katlı emülsiyonunda su damlacığı boyutunu ölçmek için kullanılmıştır. Örnekler 18 mm'lik cam tüplere yüksekliği 40 mm olacak şekilde aktarılmıştır. Δ=36. saniyede partikül boyutu 8,91 ± 0,51 μm ve Δ=66. saniyede ise partikül boyutu 10,23 ± 0,07 μm olarak ölçülmüştür. Farklı ayçiçek yağı konsantrasyonlarının (%20 su oranında) ve farklı su konsantrasyonlarının (%20, %26,67, %30, %40, %45, %60 su oranlarında) çift katlı emülsiyonların reolojik ve tekstürel karakteristikleri üzerindeki

etkisi reometre cihazında ve tekstür analiz cihazında değerlendirilmiştir. Tekstür analizi için örnekler dörderli olarak küçük plastik kutulara ortalama 20 mm yüksekliğe ulaşacak şekilde aktarılmıştır ve her bir emülsiyonun ortalama sertliği ve standart sapma değerleri bir gün sonra hesaplanmıştır. Grafik üzerinde değerlendirilen tekstür sonuçları su oranı sabitken %30'dan %55'e kadar artan ayçiçek yağı oranının sertlik değerlerini orantılı olarak düşürdüğünü göstermiştir. Sertlik değereri sırasıyla 13,40 ± 1,68 N (IV), 9,70 ± 2,13 N (V), 8,12 ± 0,70 N (VI), 3,42 ± 0,61 N (VII) olarak ölçülmüştür. Su oranının %30'den %60'a kadar yükselmesi yine çift katlı emülsiyonların sertlik değerlerinde düşüşe sebep olmuştur. Değişik su konsantrasyonlarında sertlik değerleri 58,99 ± 6,45 N (VIII), 27,47 ± 4,43 N (IX), 39,04 ± 2,13 N (X), 6,32 ± 0,67 N (XI) olarak ölçülmüştür. Ancak %20 ve %26,67 oranlarında su içeren diğer emülsiyondaki sertlik değerlerinde büyük bir fark gözlemlenmemiştir. Viskoelastik davranışı belirlemek için genlik kıvrılma gerilimi ve frekans kıvrılma testleri üçer tekrarlı olacak şekilde örnekler hazırlandıktan iki gün sonra uygulanmıştır. Emülsiyonların ve zayıf jel ve elastik özelliklere sahip olduğu tespit edilmiştir. Reolojik sonuçlar tekstür analiz sonuçlarıyla paralellik göstermiştir. Ayçiçek yağ oranı %30'dan %55'e kadar artırıldığında jel sertliği düşmüştür ve daha çok miktarda ayçiçek yağının su fazına geçtiği görülmüştür. Su oranı %20'den %60'a çıkartıldığında yine jel sertliği düşüş göstermiştir. Diferansiyel taramalı kalorimetre emülsiyonların pik sıcaklığı ve ısı akışı hakkında bilgi sahibi olmak için kullanılmıştır. Termogramlardaki pikler palm yağının çift katlı emülsiyon formu esnasında katılaştığını onaylamıştır. Belirli sürelerde 4 ˚C'de depolanan örneklerde hala çift katlı emülsiyon yapılarının korunduğu ancak su fazının bozulmaya başladığı ve emülsiyon stabilitesinde düşüş olduğu gözlemlenmiştir.

Bu çalışmanın amacı jelatin ve ksantan gam ile Y/S emülsiyonlarını stabilize etmek ve daha sonra bu emülsiyonları düşük katı yağ içeriğine sahip Y/S/Y emülsiyonlarını oluşturmak için bir temel olarak kullanmaktır. Çalışmanın sonuçları sadece doğal biyopolimerler yardımıyla ayçiçek yağının hapsedilebileceğini ve katı yağ oranının azaltılarak daha düşük doymuş yağ içeren ürünlerin üretilebileceğini göstermiştir. Ayrıca, çift katlı emülsiyonların optimizasyonunda ve formulasyonunda bu metodun kullanılması ilerideki çalışmalarda aroma maddelerinin veya diğer bileşenlerin enkapsülasyonu için bu yapının temel alınabileceğini göstermiştir.

1. INTRODUCTION

Recently, fabrication and characterization of DEs has become promising for use in food industry. Two major potential uses in industrial applications are the encapsulation of nutrients for flavor delivery and the production of reduced saturated fat products which are healthier (Dickinson 2011).

Fats and oils constitute one of the main classes of foods. Either they are naturally present in foods or they are added as ingredient for functional benefits and they also have an important role in human diet. However, saturated fats are considered to be unhealthy and have been found to show negative effects on health in terms of cholesterol profiles (Marangoni and Garti, 2011; List et al, 2007). Due to these concerns, researchers currently focused on seeking alternatives to structure a form of liquid oil aiming to reduce saturated fat or trans-fat in food products (Patel and Dewettinck, 2015). In this case, a new approach based on the use of O/W/O DE's can be considered as promising option. However, the preparation and characterization of these DEs are more difficult than simple emulsion because they are thermodynamically unstable. For this reason they have a tendency to flocculate and creaming (Aserin 2008; Benichou et al, 2007). Emulsions are formed in the presence of surface active agents such as emulsifiers. Proteins have hydrophilic and hydrophobic parts that become integrated when there is a water–oil or oil–water interface in order to lower their interfacial tension which makes them natural emulsifiers (Wilde et al, 2004). The problem of stability can be solved by surface active proteins due to their environmentally friendly features such as biodegradability. However, proteins are unable to form liquid oil due to the their limited dispersibility in oil. However, researchers have found that protein-polysaccharide matrices are appropriate food structurants that can be used for the encapsulation of liquid oils (Benichou et al, 2007; Patel et al, 2015).

According to our findings, more than one synthetic surface active agents were used in previous researchs and they were high in amount to provide stability in DEs. However, petroleum based sources are strongly restricted by food organizations. For

this reasons, in the present work, a novel structured liquid oil system is developed to lower the saturated fat content of a conventional food emulsion by replacing it with an equivalent O/W/O emulsion. The current study is based on a two-step process; in the first step, a concentrated oil-in-water emulsion was prepared which was stabilized by the surface active protein (GL) and the non-surface active polysaccharide (XG). In the second step, hardstock was added to oil-in-water emulsion and then the mixture was subjected to low temperature cooling to form a DE system. These systems have a strong potential in encapsulating oils and they can be processed in food applications to reduce saturated fat compounds.

1.1 Purpose of Thesis

Margarine is an example of water-in-oil food emulsion which contains 20 wt% aqueous phase and 80 wt%. fat phase. The fat phase consist of liquid oil and hardstock. If some of the liquid oil can be transferred in the internal water droplets then less crystalline fat would be needed to get a similar structure (Figure 1.1).

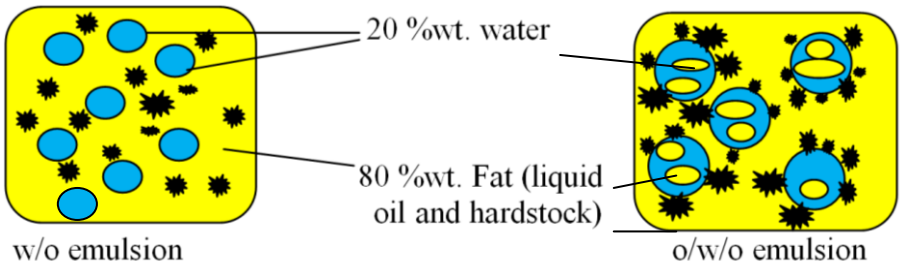

Figure: 1.1: Schematic structures of primary and double emulsions.

The main objective of the proposed research is to focus on the use of biopolymers such as GL and XG to stabilize water continuous emulsions and further use these emulsions as a template to generate O/W/O emulsion with low solid fat content.

The specific objectives of this thesis study are:

a) To formulate O/W/O DEs at different proportions of liquid oil, hardstock and water by crystallization of fat phase,

b) To characterize the DEs in terms of their texture, rheology, thermal stability, droplet size distribution and microscopic structures.

1.2 Literature Review

1.2.1 Double emulsions

DEs, also known as multiple, multiplex or multilayered emulsions are the emulsions in which the dispersed phase itself is an emulsion in form of fine droplets. DEs includes two types: oil-in-water-in-oil (O/W/O) and water-in-oil-in-water (W/O/W) (Figure 1.2). In an O/W/O type emulsion, O_1 and O_2 constitute an internal oil phase and an external oil phase, respectively. There are two different interface layers: O_1-W layer which surrounds internal oil droplets and W-O_2 layer surrounds water droplets. On the other hand, in W/O/W type, water droplets are located within oil droplets which are dispersed within a continuous water (Lamba et al, 2015).

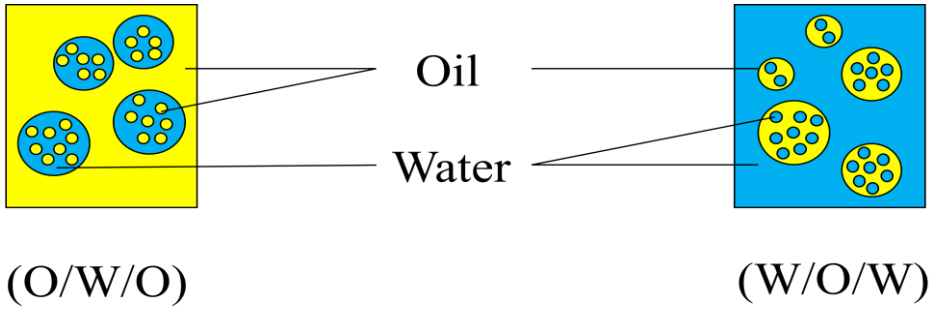

Figure 1.2: Schematic representation of oil-in-water-in-oil and water-in-oil- in-water emulsions.

1.2.2 O/W/O double emulsion formation

DEs were prepared with two major methods so far: one-step double emulsification and two-step double emulsification. 'One-step' process involves heating which causes phase inversion (Pradhan and Rousseau 2012; Sajjadi et al, 2003). In 'two-step' process, the first step is preparing the PE: an oil and a water phase are homogenized together in the presence of a water-soluble emulsifier to form an O/W emulsion. In the second step, the O/W emulsion is homogenized with an oil phase in the presence of an oil-soluble emulsifier to form an O/W/O emulsion (Kumar et al, 2012; O' Dwyer et al, 2013).

So far the use of high shear devices and membrane emulsification are the two procedures for DE preparation. Ultrasonicator, high pressure homogenizer, microfluidiser and high shear mixer such as Ultraturrax are the devices used for the formation of stable DEs. These devices work on the principle of high shear produced

by turbulence, cavitation and collision which leads to the breakdown of the droplets and uniform dispersion of the continuous phase. For example; the formation of PE requires high shear rate, however a slower shear rate is necessary in order to avoid the break of the DE structure (Lamba et al, 2015).

1.2.3 Inner and outer oil phase in double emulsions

O/W/O DEs intended for food formulations usually have vegetable oil as oil phase. Rapeseed oil, (Edris and Bergnståhl, 2001) hydrogenated palm kernel oil (Cho and Park, 2003), palm-sunflower oil blend (O'Dwyer et al, 2013) and palm stearin-cotton blend (Jahaniaval et al, 2003) were used as outer oil phase to form O/W/O DEs until now.

The palm oil is extracted from oil palm (*Elaeis guineensis*) fruits. The fruit consists of an outer skin (exocarp), a flesh (mesocarp) and a kernel containing palm kernel oil (Poku, 2002). It has approximately 50% saturated and 50% unsaturated fatty acids. The fatty acid distribution within the triaclylglceride (TAG) molecules plays an important role in determination of the polymorphic behavior of the fat. Palm stearin, being a higher-melting fraction, contains more saturated fatty acid when compared with palm oil and it is solid-like at room temperature (Lin, 2002).

1.2.4 Applications of o/w/o double emulsions

Due to some difficulties there are only few researches attempting to generate O/W/O emulsions in the food field (Table 1.1). Main applications include the encapsulation of flavors or substances. Researchers have investigated encapsulated fish oils with the help of sodium caseinate (O'Dwyer et al, 2013) and wheat gluten (Liao et al, 2012). Native polysaccharides are non-surface active except for gum arabic which contains glycoproteins, acetylated pectin and some galactomannans. Cho and Park (2003) encapsulated five different flavor components with the help of arabic gum-maltodextrin complex solution for the stabilization of the internal oil–water interface of O/W/O emulsions. Benichou et al. (2007) have described the stabilization of the oil–water interface of DEs by complexes of whey protein isolate-xanthan gum and whey protein isolate-fenugreek gum.

Table 1.1: Potential applications of O/W/O DEs in the food industry.

Inner O_1 Phase	Water Phase Emulsifier/Stabilizer	Outer O_2 Phase Emulsifier/Stabilizer	Encapsulates	Method	Reference
Rapeseed Oil	Lactose and caseinate	Rapeseed oil and PGPR	Orange Oil (80%)	Spray Drying (O/W/O/W)	Edris and Berhnstahl (2001)
Rapeseed Oil	Gum arabic and maltodextrin	Hydrogenated palm kernel oil and blend of PGPR and Span 80	Flavor Components (20%)	Microfludisation (Ethanol used as dehyrating agent)	Cho and Park (2003)
a)Camelina Oil b) Fish Oil c) Camelina and fish oil blend	Salt and sodium caseinate	Palm oil and sunflower oil blend PGPR and β-carotene	Omega-3 rich oil	Conventional lipid oxidation methods Homogenization	O'Dwyer et al. (2013)
Succinic acid deamidated wheat gluten-Fish oil	PEG 300	Span 80 was added to the mineral oil solution at 1%	Fish oil-mineral oil	Heating-crosslinking & solvent evaprotaion	Liao et al. (2012)
Liquid canola oil	Sodium caseinate and lecithin	Palm-cotton stearin	Canola oil	Fat Crystallization Mixing two (O/W) emulsions together	Jahavanial et al. (2003)
Corn oil	Whey protein-potato starch polymer mixture	Tween 80, Span 80	β-carotene	Ultrasonic emulsification. Oxidized starch solidified by Fe^{3}+ with cross-linking method	Wang et al. (2015)

They claimed that it may have potential applications in food products. O/W/O DEs stabilized with lactose-caseinate mixtures (Edris and Bergnståhl, 2001) and whey protein-potato starch polymer mixture (Wang et al, 2015) have been also studied in the literature.

1.2.5 Technological challenges and stability issues

The stability of DE is affected by its composition and emulsification methods used. Furthermore, various parameters need to be considered during the preparation of O/W/O DEs such as applied shear speed, temperature during homogenization, the amount and type of emulsifier, the proportion of oil and water phases, the final droplet size etc. (Lamba et al, 2015).

Stability of PE is important for the overall stability of the DE. A stable emulsion is the one with no observable changes over time in terms of size distribution of droplets and the state of aggregation. Stable emulsion can be defined in terms of encapsulation efficiency, encapsulation stability and sedimentation stability. Encapsulation efficiency is defined as the amount of intact internal phase particles present in the DE after a stipulated time interval. Encapsulation stability refers to the reluctance of DE, in changing the encapsulation efficiency on application of destabilizing agents such as centrifugal speed or high temperature. Sedimentation stability determines the structural integrity of the multiple emulsions and it is measured as the ratio of the sediment height to total height of the emulsion in measuring cylinder (Sapei et al, 2012).

Despite the immense potential for application of DE there is a problem: The preparation and characterization of DE are more difficult compered with simple emulsions because their stability is more challenging to maintain (Muschiolik and Bunjes, 2007). The three major instability mechanisms are represented schematically in Figure 1.3. Mechanism A shows the coalescence in which two droplets merge into one bigger droplet after collisions. Mechanism B is the coalescence between the smaller inner droplets within the oil globules. Mechanism C is the coalescence of the small inner droplets with the outer droplets interface which leads to the transfer of some internal droplets to the external continuous phase. These mechanisms are occurring simultaneously and all contribute to the overall rate of destabilization of the DE (Dickinson 2011).

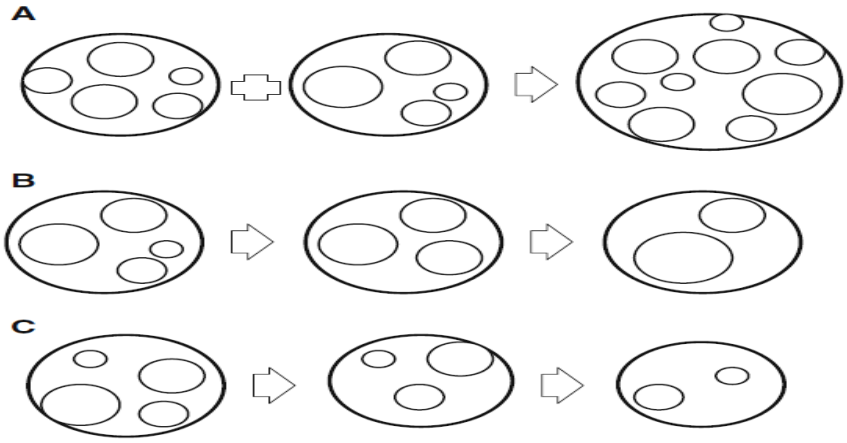

Figure 1.3: Schematic representation of the main breakdown mechanisms of a DE. (A) outer droplet coalescence; (B) inner droplet coalescence; (C) transfer of some internal droplets to external phase (Dickinson 2011).

1.2.6 Effects of emulsifiers in emulsions

Emulsifiers have amphiphilic properties containing both hydrophilic and lipophilic parts that can gather in interfacial area. They lower surface tension and stabilize two immiscible liquids in an emulsion. Their amount affects the emulsion properties, as lower amounts may result in unstable system, whereas higher amounts may also lead to destabilization (Davis and Walker, 1987). A combination of hydrophilic and hydrophobic emulsifiers is usually employed to stabilize multiple emulsions. As polymeric emulsifiers are complex molecules with high molecular weight, their tendency to migrate is very slow. They form a bulky viscoelastic layer around droplets preventing the release of encapsulated material and also provide steric stabilization which prevents coalescence of internal droplets and thus improves stability.

Hydrophobic emulsifiers with a hydrophilic-lipophilic balance (HLB) value of four or less are used to emulsify water droplets in the oil phase. They have higher proportion of nonpolar groups and hence are soluble in the oil phase. The polyglycerol-polyricinoleate (PGPR), obtained from castor beans, has been demonstrated to be highly effective for stabilizing food based DEs. It acts as a bridging agent and a modifier between fat crystals and helps adsorption at oil-water interface. PGPR is used to improve the flow properties in chocolate and vegetable fat coatings. However, the use of these kind of emulsifiers is restricted by food organizations. These limitations led researchers to investigate alternative ways to overcome the requirement of synthetic emulsifiers. Therefore, the point of attention

has turned towards using the advantage of the functional role of natural biopolymers such as proteins and polysaccharides in DE formulations (Dickinson, 2011).

1.2.7 Stabilization of o/w/o emulsions by hydrocolloids

The hydrocolloids are a macromolecules (proteins and polysaccharides) that is water soluble or hydrophilic polymers that form colloid when dispersed in water. The colloids are homogeneous systems that have the characteristics of a solution and also a suspension because their one phase is dispersed into another unlike solution where the phase is molecularly dissolved.

Compared with small-molecule emulsifiers, hydrocolloids are much less susceptible to diffuse and migrate between phases. Furthermore, hydrocolloids can be used as effective stabilizers of the water–oil interface of emulsion droplets because of their ability to stabilize network structures in the dispersed and the continuous phases (Patino and Pilosof, 2011; Dickinson, 2011). These benefits make hydrocolloids promising ingredients for food-based applications to reduce the use of synthetic emulsifiers.

1.2.7.1 Protein–polysaccharide conjugates for stability

In recent years protein-polysaccharide complexes have been gaining much more attention for stabilization of food-grade DEs (Bouyer et al, 2012). Previous studies have shown that conjugates of protein and polysaccharide have a synergistic effect on the functionality of the DE (Benichou et al, 2007; Li et al, 2012). It is explained by a formation through a Maillard-type reaction which allows the formation of amide linkages. This causes stability of possible changes in pH, ionic strength and temperature (Dickinson and Euston 1991; Schmitt et al, 1998). Such mixtures improve the emulsion stability (Lam and Nickerson, 2013), decrease the release rate from water phase (Benichou et al, 2004) and prevents creaming, flocculation and coalescence of droplets (Dickinson, 1991, p.132-146).

1.2.7.2 Xanthan gum and gelatin interactions

An extracellular polysaccharide, XG obtained through fermentation based on the culture, in aerobic conditions from *Xanthomonas campestris*. Its industrial importance is based on its ability to control the rheology of the water based systems.

XG solutions shows a high viscosity even at a low concentration in comparison with the other polysaccharide solutions. It has become a very effective thickener and emulsion stabilizer because of this property (Hee et al, 2008).

Gelatin, a proteinaceous substance, was mainly obtained from animal connective tissue and was produced by either acidic conditions or alkaline conditions. The main animal sources for GL are processed from skins or bones of beef, pork fish skin and poultry. It is widely used for multifunctional properties such as gel formation, thickeners, foaming, film formation elasticity water binding and emulsification (Imeson, 2011).

The effect of GL and XG interactions was proved by non-coulombic interactions with the involvement of NH and OH groups, as well as hydrophobic reactions (Lii et al, 2002). It has been proved that the combination of XG and GL helps the modification of the microstructure of the emulsions. Adding XG strengthens the protein network formed by adsorbed protein molecules at the oil interface (Patel et al, 2015).

1.2.8 Crystallization of fat phase to improve stability

In an O/W emulsion, water represents continuous phase but dispersing of O/W emulsion in another oil or fat is not easy because of differences in their polarity, wettability and surface tension. Furthermore, DEs are more susceptible to breakdown in a time compared to PE. Fat crystallization technique can be used to improve the stability of the O/W/O DE as it ensures stability, firmness and overrun (Jahaniaval et al, 2003). The crystallization involves following basic steps:

1) Generation process of a super saturation state: Solutes dissolved above the saturated concentration by heating followed by cooling it in order to achieve super saturation.

2) Primary crystallization: formation of crystalline lattice from solution.

3) Secondary crystallization: the growth of crystals until the equilibrium is obtained.

4) Re-crystallization: A reorganization of the crystalline structure to a lower the energy state (polymorphism, Ostwald ripening, agglomeration and contraction),

generally without any change in the amount of crystalline phase volume (Bayés-garcía et al, 2015; Patel and Koen, 2015).

Jahaniaval et al. (2003) stabilized O/W/O with low solid fats by crystallizing the fat with plastic properties (cotton-palm stearin) at a low temperature. They used O/W emulsion which includes completely liquid fat and the other includes both liquid and plastic fat to form O/W/O with low solid fat content.

1.2.9 Characterization of double emulsion properties

1.2.9.1 Viscosity

Viscosity can be described as the measure of the internal friction of a fluid. This friction occurs when a layer of fluid is moved to another layer. The force required for this movement is called shear. Shearing occurs when the fluid is physically moved by spreading, spraying or mixing. Higher force is necessary to move high viscous liquids compared to less viscous liquids (Lamba et al, 2015). Moreover, emulsions shows non-Newtonian behavior. Their viscosity decreases as shear rate increases which is the shear thinning behavior. Viscosity plays a vital role in the application of DE in food products and it is measured at a specific temperature using rheometer.

Rheology is an commonly used method, which allows defining particle charge, colloidal interactions and the dispersed phase volume fraction (Clausse et al, 2005). The water and oil proportion of the DE, the amount of emulsifier (Prakash, 2012) processing parameters like pressure (Kumar, 2011) all have an effect on the rheology of the system. Viscosity of the solution tends to decrease with longer periods of storage time of inner phase content's release and it causes increase in creaming (Lutz et al, 2009).

G' is a storage modulus or elastic (solid-like or energy storing) which measures the stored energy representing the elastic portion and the G" is a loss modulus or viscous (liquid-like or energy dissipating) properties measures the energy dissipated as heat representing the viscous portion. While G' > G'' indicates the solution has more elastic behavior, G''> G' highlights a solution with more viscous behavior (Steffe 1996).

1.2.9.2 Droplet size

Droplet size is another important parameter in DE. After storing emulsion, the measurement of emulsion particle size at certain times gives information about emulsion stability (O'Regan and Mulvihill 2009a). For encapsulation applications, size of the internal water droplets in the O/W/O DE should be small but they should be a lot in number and also equally distributed. The small water droplets show better stability.

Devices like Ultraturrax produce particles in micrometric size, whereas the high-pressure homogenizer, the sonicator and the microfluidiser produce nano-sized DEs. Particle size of DE is affected by the processing conditions such as temperature, time, inner phase ratio and the type of surfactant. Varying the viscosity ratio also showed an effect on surface mean diameter of the particles (Frank et al, 2011; Lamba et al, 2015).

There are various methods to determine the droplet size. In this study, static light scattering method is used for PEs, and pulsed field gradient nuclear magnetic resonance (pfg-NMR) method is used for DEs in order to measure the droplet size. Volume weighted particle size distribution is defined using static light scattering method. Particle contribution in this distribution is proportional to its $(size)^3$ or volume. Mean, mode or median statistical parameters are used to evaluate these distributions. They are used to get information about one value of particle size which can represent the distribution of all particles (Lamba et al, 2015). Generally, volume weighted mean (d_{43}) and surface area weighted mean (d_{32}) are used for qualifying the mean of the distribution of the particle sizes. (d_{32}) is related with the distribution of finer particles but (d_{43}) is related with the distribution of larger particles (Malvern Instruments 2012, Lamba et al, 2015). Pfg-NMR is one of the fastest and most non-destructive methods used for structural characterization of the emulsions (Van Duynhoven et al, 2002) and it measures the translational diffusion. According to Murday/Cotts (Murday and Cotts, 1968), pfg-NMR data of emulsions can be described by a model to determine droplet size distribution. Bernewitz et al. (2014) have made progress in the droplet size determination of /O/W/O DEs using pfg-NMR.

1.2.9.3 Thermal stability

Stated before, DEs are not stable for long time periods and their morphology can change easily. This change is explained by temperature variations, melting or freezing of the emulsion. Melting temperature of the palm influences DEs functional properties. Freezing, is the result of nucleation, which is another important parameter to note. None of the droplets freezes at the same point. So, their freezing temperatures can be different. It has been stated that the transfer of a matter can occur from undercooled droplets to already frozen droplets. The transfer will cause change in the droplet size, and also in their morphology since a smaller droplet size means lower freezing temperature. Differential Scanning Calorimetry (DSC) is suitable for obtaining information about freezing and melting temperatures, matter transfer, droplet size and emulsion stability. DSC measures the differences in the heat flux between a sample and a reference. It is easy, rapid and requires only a small amounts of sample. (Clausse et al, 2005). Observations of O/W/O systems with DSC are reported in the literature (Avendano-Gomez et al, 2005).

1.3 Hypothesis

This study was set out to test following hypothesis in emulsion systems. Development of emulsions with SFO by using GL as the emulsifier and XG as the stabilizer. Then, adding hardstock (palm oil) to PE and homogenization of mixture by a high shear mixer. It is assumed that during homogenization subjecting mixture to low temperature cooling procedure can lead to crystallization of palm oil. Fat crystalls will prevent collision of internal water droplets. Thus, formation of the DE systems with better stability will be provided.

2. MATERIALS AND METHODS

2.1 Materials

GL type B, mol wt ~50 000 (Sample No 315-0807), was received from PB Gelatins, GmbH member of Tessenderlo group (Belgium). XG (SATIAXANE CX 801 LOT R253544) was purchased from Cargill (France). Polyglycerol polyricinoleate (GRINDSTED® PGPR) was received from DuPont Nutrition & Health (Denmark). Nile red was purchased from Sigma-Aldrich Inc. (USA). SFO was obtained from Vandemoortele R&D (Izegem, Belgium). Solid fat (100 % palm oil) was provided by Vandermoortele N.V. (Izegem, Belgium) and was melted in oven at 50 ˚C before use. Distilled water was used in all experiments. Ultraturrax-T 25 Digital S25KV and Ultraturrax-type T 25 B equipments were purchased from IKA-WERKE GMBH & CO. KG (Germany).

2.2 Methods

2.2.1 Preparation of samples

Firstly, stock solutions of GL at 10 %wt and XG at 2 %wt were prepared by weighing polymer powders in distilled water. After powders were completely dispersed, accurate amount of solutions were taken in plastic container. Then SFO and stock solutions were emulsified using Ultraturrax. Three kinds of O/W PE were prepared at ratios of 6:4 (I), 2:8 (II) and 1:9 (III). The homogenization time was optimized to 3 minutes for Ultraturrax-type T 25 B, whereas it was fixed to 5 minutes for Ultraturrax-T 25 Digital S25KV. For DE preparation, in the first step, an accurate amount of PE was transferred to another plastic container and palm oil (melted at 50 ˚C) was added on to it. The mixture was homogenized again by using Ultraturrax. Under continuous shear, metallic beaker which contained ice was inserted under the container at the second minute. Thus, palm oil was subjected to low temperature cooling below 0 ˚C to form O/W/O DEs. As the oil-water proportion changed for each sample, homogenization time varied from 9 to 18

minutes. Schematic representation of the preparetion process of an O/W emulsion and incorporation of palm oil which results in the formation of an O/W/O DE is presented in Figure 2.1. Additional drawings are included to explain the microstructure of depicted samples. The interface of the yellow emulsion droplet shows an adsorbed layer of GL (red dots) and sheets of XG (curved green lines).

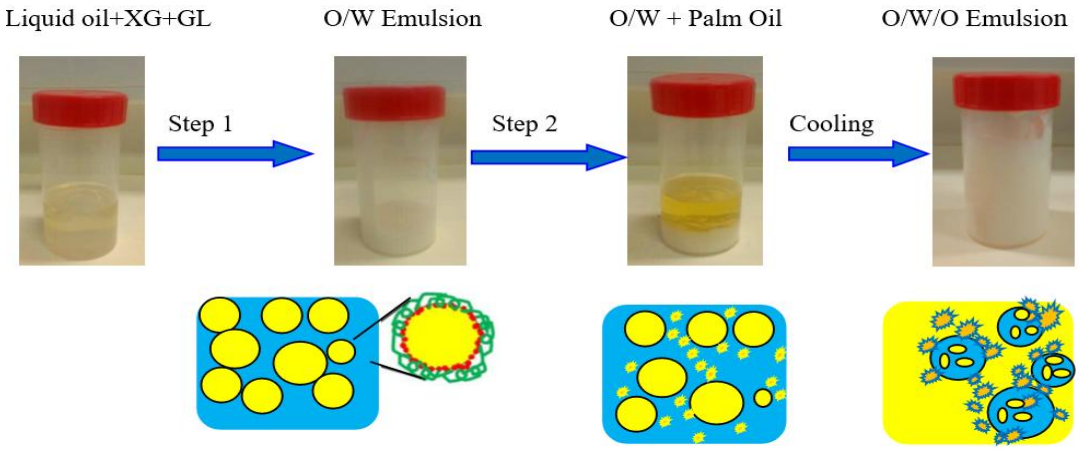

Figure 2.1: Photographs and schematic representations of the process to prepare a O/W emulsion (Step 1) followed by the addition of palm oil (Step 2) then cooling below 0 ˚C under shear.

DEs were prepared in three different ways. In the first one, O/W ratio of 6:4 PE (I) was prepared from 36 g SFO, 18 g XG solution and 6 g GL solution. 30 g of SFO-palm blend were added to 30 g PE. Oil continuous emulsions were prepared by emulsifying melted palm oil with SFO (IV, V, VI, VII) at different amounts (Table 2.2). The second type of emulsions (VIII, IX, X, XI) consist of four blends with an increasing amount of the 2:8 O/W ratio PE (II) (Table 2.3). 2:8 O/W ratio PE (II) prepared from 12 g SFO, 42 g XG solution and 6 g GL solution. For sample XI, 15 g of oil blend (containing 14.76 g palm oil and 0.24 g PGPR) was added to 45 g PE. The third type involves two blends of emulsion samples (XII, XIII) that are based on the increasing amount of sample I (Table 2.4). For the emulsions IV, V, VI, VII Ultraturrax-type T 25 B was used and for emulsions number VIII, IX, X, XI, XII and XIII Ultraturrax-T 25 Digital S25KV was used during emulsification.

2.2.1.1 Primary emulsions with different oil-water concentration

Proportion of XG, GL and SFO in PEs were presented in Table 2.1. GL concentrations of all PEs were 1%. XG and GL concentrations indicate the amount in the total PE.

Table 2.1: Proportion of polymers and SFO in PEs.

PE	Oil Phase (SFO) (%)	Water Phase(%)		
			XG (%)	GL (%)
I	60	40	0.6	1
II	20	80	1.4	1
III	10	90	1.6	1

2.2.1.2 Double emulsions at constant water concentration

A fixed amount of sample I (30 g) was used to structure DEs at constant water concentration. 30 g palm oil-SFO blend added to sample I. Consequently, all DEs contained 20 wt% water phase. DE table with constant water concentrations presented in Table 2.2. XG and GL concentrations indicate the amount in the total DE**.** XG and GL concentrations of all DEs were 0.3% and 0.5%, respectively**.**

Table 2.2: DE table at constant water concentrations. O/W ratio of 6:4 PE emulsion (I) was used for DE structuring.

DE	Oil_1 SFO (%)	Water Phase XG+GL Solution (%)			Oil_2 Palm Oil (%)
			XG (%)	GL (%)	
IV	30	20	0.3	0.5	50
V	38.3	20	0.3	0.5	41.7
VI	46.7	20	0.3	0.5	33.3
VII	55	20	0.3	0.5	25

2.2.1.3 Double emulsions at different water concentrations

A different amount of (22.5 g, 30 g, 33.75 g and 45 g) sample II was used to structure DEs at different water concentrations. 37.5 g, 30 g, 22.25 g and 14.76 g palm oil was added to sample II respectively. DE table with different water

concentrations were presented in Table 2.3. XG and GL, palm oil and SFO concentrations indicate the amount in the total DE**.**

Table 2.3: DE table with different water concentrations. O/W ratio of 2:8 PE (II) was used for DE structuring.

DE	Oil_1 SFO (%)	Water Phase XG+GL Solution (%)	XG (%)	GL (%)	Oil_2 Palm oil(%)	PGPR(%)	Storage (days)
VIII	7.5	30	0.525	0.375	62.5	0	7 at 4 ˚C
IX	10	40	0.7	0.5	50	0	60 at 4 ˚C
X	11.25	45	0.782	0.558	43.75	0	14 at 4 ˚C
XI	15	60	1.05	0.75	24.6	0.4	40 at 4 ˚C

For third type of DE, PE was prepared again from sample I. 30 and 40 g of PE from sample I was used for DE structuring. DE table with different water concentrations were presented in Table 2.4. XG, GL, SFO and palm oil concentrations indicate the amount in the total DE**.**

Table 2.4: DE table with different water concentrations. O/W ratio of 6:4 PE (I) was used for DE structuring.

DE	Oil_1 SFO (%)	Water Phase XG+GL Solution (%)	XG(%)	GL(%)	Oil_2 Palm oil (%)	Storage (days)
XII	30	20	0.3	0.5	50	40 at 4 ˚C
XIII	40	26.67	0.4	0.67	33.33	40 at 4 ˚C

2.2.1.4 Effect of homogenization duration during emulsification

Fixed homogenization duration for each PE presented in Table 2.5.

Table 2.5: Fixed homogenization durations for PEs.

PE	Homogenizer brand (Ultraturrax)	Time PE (minute)	Rotation per minute
I	T 25B	3	11000
II	T 25B	3	11000
III	T 25B	3	11000
I	T 25 Digital S25KV	5	11000
II	T 25 Digital S25KV	5	11000
III	T 25 Digital S25KV	5	11000

Fixed homogenization durations for each DE presented in Table 2.6. Mixtures were subjected to cooling after two minutes.

Table 2.6: Fixed homogenization durations for DEs.

DE	Homogenizer brand (Ultraturrax)	Rotation per minute (rpm) and time (minute)	
IV	T 25B	11000 rpm 2 min	13000 rpm 6 min
V	T 25B	11000 rpm 2 min	13000 rpm 6 min
VI	T 25B	11000 rpm 2 min	13000 rpm 6 min
VII	T 25B	11000 rpm 2 min	13000 rpm 6 min
VIII	T 25 Digital S25KV	8000 rpm 6 min	4000 rpm 4 min
IX	T 25 Digital S25KV	8000 rpm 6 min	4000 rpm 4 min
X	T 25 Digital S25KV	8000 rpm 6 min	4000 rpm 4 min
XI	T 25 Digital S25KV	8000 rpm 6 min	4000 rpm 12 min
XII	T 25 Digital S25KV	8000 rpm 6 min	4000 rpm 3 min
XIII	T 25 Digital S25KV	8000 rpm 6 min	4000 rpm 3 min

2.2.2 Microstructure studies

2.2.2.1 Optical microscopy

Optical microscopic analysis (under normal light and polarized light) were conducted by the use of Leica DM2500 microscope (Leica Microsystems, Wetzlar, Germany). A drop of emulsion sample was settled on a microscope slide, and then, it was covered with a cover slip. The slides were placed on the temperature-controlled plate to visualize the microstructure at 20 ˚C. The estimated sizes of the particles from the obtained images were recorded with a color camera Leica MC170 HD. In order to see how DEs were affected after storage, samples were kept in at 4 ˚C and images were recorded at different storage times.

2.2.2.2 Cryogenic scanning electron microscopy

The emulsion samples were placed in the slots of a stub, plunge-frozen in liquid nitrogen. Firstly, samples were freeze-fractured and transferred into the cryo-preparation chamber (PP3010T Cryo-SEM preparation system, Quorum Technologies, UK). Water was sublimated in the cryo-preparation chamber. Then samples were subsequently sputter-coated with Pt and were examined with a JEOL JSM 7100F SEM (JEOL Ltd, Tokyo, Japan) to study their microstructure.

2.2.3 Rheological measurements

The rheological measurements of the emulsions were carried out on an advanced rheometer AR 2000 ex (TA Instruments, USA) equipped with a Peltier system. A parallel plate cross-hatched geometry of 40 mm diameter was used. Experiments about the rheology of the samples depended on the oil-water concentrations. Experiments including the amplitude sweeps (stress from 1 Pa to 5000 Pa, frequency = 1 Hz) and frequency sweeps (frequency from 0.1 to 100 Hz, stress from 2 Pa to 25 Pa) were carried out at 20 ˚C and 10 ˚C. To study the effect of GL and XG concentrations on the structural properties, rheological measurements were conducted on three replicates two days after their preparation.

2.2.4 Fracture studies

The examination of large deformation fracture of DE samples was carried out using an A 5942 Instron TA 500 texture analyzer (Lloyd Instruments, Bognor Regis, West Sussex, UK). The samples were filled in plastic tubes and stored at 4 ˚C in a thermostatic cabinet. The examination of large deformation fracture was carried out on the samples after one day storage. An 11-mm-diameter cylindrical probe was penetrated ino the sample to a depth of approximately 20 mm at a rate of 1 mm/sec with 0.1 N trigger value. The measurements were conducted on four replicates of each sample. The hardness values were determined by measuring the mean and standart deviation (SD) values of replications.

2.2.5 Thermal behaviour

The melting profile of the components in the DEs was analyzed after two weeks of preparation in triplicate using Q1000 Differential Scanning Calorimeter (TA Instruments, New Castle, DE). The DSC was calibrated with indium (TA Instruments, New Castle, DE), azobenzene (Sigma-Aldrich, Bornem, Belgium) and undecane (Acros organics, Geel, Belgium) before the analysis. 5 to 10 miligrams of samples were sealed in hermetic pans and an empty pan was used as a reference. The results of the DSC profile curves from 6 ˚C to 95 ˚C were obtained by using TA Universal Analysis software. The temperature of the peaks were founded by integrating peak on linear direction. The results were given as the mean and SD values of two replications.

2.2.6 Primary emulsion particle size distribution

The particle size distribution (PSD) of emulsions samples was analyzed using a Malvern Mastersizer 3000 (Malvern Instruments Ltd, Malvern, Worcestershire, UK). This analysis was based on laser light scattering. By comparing the scattering pattern of the sample PSD's was calculated to Mie theory with a mathematical inversion process. 1 gr samples were dissolved in 100 g of water (1:100 dilutions) and then measured in triplicates. All measurements were carried out at 20 ˚C.

2.2.7 O/W/O double emulsion particle size distribution

The water droplet size analysis of O/W/O emulsions was measured by pfg-NMR. The samples were analyzed at 5 ˚C to minimize inter droplet water diffusion (Van lent et al., 2008). NMR measurements were performed on a benchtop Maran Ultra spectrometer (Oxford Instruments, UK) running at a frequency of 23.4 MHz. The samples were filled in 18 mm diameter glass NMR-tubes (Oxford Instruments, UK) for a height of about 40 mm. A Teflon spacer of 27 mm was used so that the particle size was measured on the sample volume between 0 mm and 20 mm height.

The Murday Cotts model was applied to fit the water diffusion data, which estimates the arithmetic mean droplet radius (R_{43}) and arithmetic standard deviation (σ) of the lognormal volume-weighted droplet radius distribution. The diffusion coefficients D of the bulk water phase and of the water in the O/W emulsion were measured using the DSD script (Oxford Instruments, UK) and varying the duration (δ) between 0.05 and 2.75 ms while keeping G and Δ constant at 0.14 T/m and 200 ms, respectively.

The water diffusion signals of three repetition tubes of 30/20/50 O/W/O emulsions were measured at (a) Δ=0.36 second and at (b) Δ=0.66 second. The experiments were conducted using an inversion recovery-stimulated echo pulse sequence characterized by a time duration τ (i.e. T_1-filter) and with this it was possible to suppress the NMR contribution of the fat phase. Using the bulk O_1-phase, the τ-value associated with minimum oil signal was measured as 60000 µs. In order to check the efficiency of the T_1-filter in eliminating the oil signal contribution from the oil phases to the water diffusion signal, the first I_0 (at G=0 T/m) and last echo intensity I (at G= 2 T/m) were measured using Δ=360 millisecond and τ=60000 microsecond. In comparison to $1.0\cdot(I/I_0)$=1600/3000 for the 30/20/50 O/W/O emulsion, the $0.3\cdot(I/I_0)$ for the O_1 and

$0.5 \cdot (I/I_0)$ for the O_2-phase measured as 61.2/99 and 12.9/13.6. Hence, the applied T_1-filter was sufficient for the removal of both oil phase signal contributions.

2.2.8 Statistical analyses

Hardness results, droplets size results and thermal properties were analyzed by IBM SPSS Statistics Program (21^{th} version) by using one way analysis of variance (ANOVA) at 0.05 significant level and Tukey's New Multiple Range Test was applied as post hoc test. The differences between all samples, were evaluated statistically. Tukey's range test was applied to exact values to observe the differences between samples ($p<0.05$). The results were reported as mean value ± SD. Statistical analysis results of samples were given at Appendix A, B and C.

3. RESULTS AND DISCUSSION

3.1 Characterization of Primary Emulsions

3.1.1 Optical microscopy

GL and XG formed O/W emulsion when used together. This observation could be explained by non-covalent interactions between GL-XG leading to enhanced stabilization of emulsion due to the stiffening of the interface and viscosity enhancement of the continuous phase. A drop of freshly prepared emulsion sample was placed on a slide, a cover slip was added and then, an equal amount of pressure was applied on these samples to record their structure under optical microscopy. Emulsions represent sample I (a, b) 6:4 of O/W, sample II (c, d) 8:2 of O/W, sample III (e, f) 9:1 of O/W respectively (Figure 3.1). Notice the network of GL-XG around oil droplets marked by red arrows. Ultraturrax-type T 25B was used for emulsion preparation. Oil droplets were observed as solid round particles in non-polarised light microscopy representing a dispersed phase. The gray patch around these oil droplets represents the water as aqueous continuous phase. It could be observed that networks of polymers around oil droplets are thicker when the XG concentrations increase from 0.6 to 1.6 wt% at constant GL ratio (1 wt%). Furthermore it is observed that there were less SFO droplets in amount at 90 wt% water when compared with 40 wt% water.

3.1.2 Cryogenic scanning electron microscopy

The samples were studied at cryogenic (liquid nitrogen) temperatures to record the network of polymers in the bulk phase and at the droplet interface. Cryo-SEM has the ability to remove surface water (ice) by controlled specimen sublimation. The freeze fractured samples of the emulsion were subjected to sublimation in the cryo-preparation chamber in order to remove all of the water. Ultraturrax-T 25 Digital S25KV was used for the emulsion preperation. As seen in Figure 3.2a and Figure 3.2b, oil droplets interconnected via a network with a distinct layer of polymers (GL

and XG) after the removal of water phase. With a closer look, image c and d shows the network of polymers in the bulk phase and the presence of distinct interfaces (indicated by red arrows). The layer of polymers around the oil droplets is responsible for preventing the coalescence of the oil droplets. Red arrows indicates that increase in the XG concentration resulted in thicker network in the bulk phase and at the interfaces.

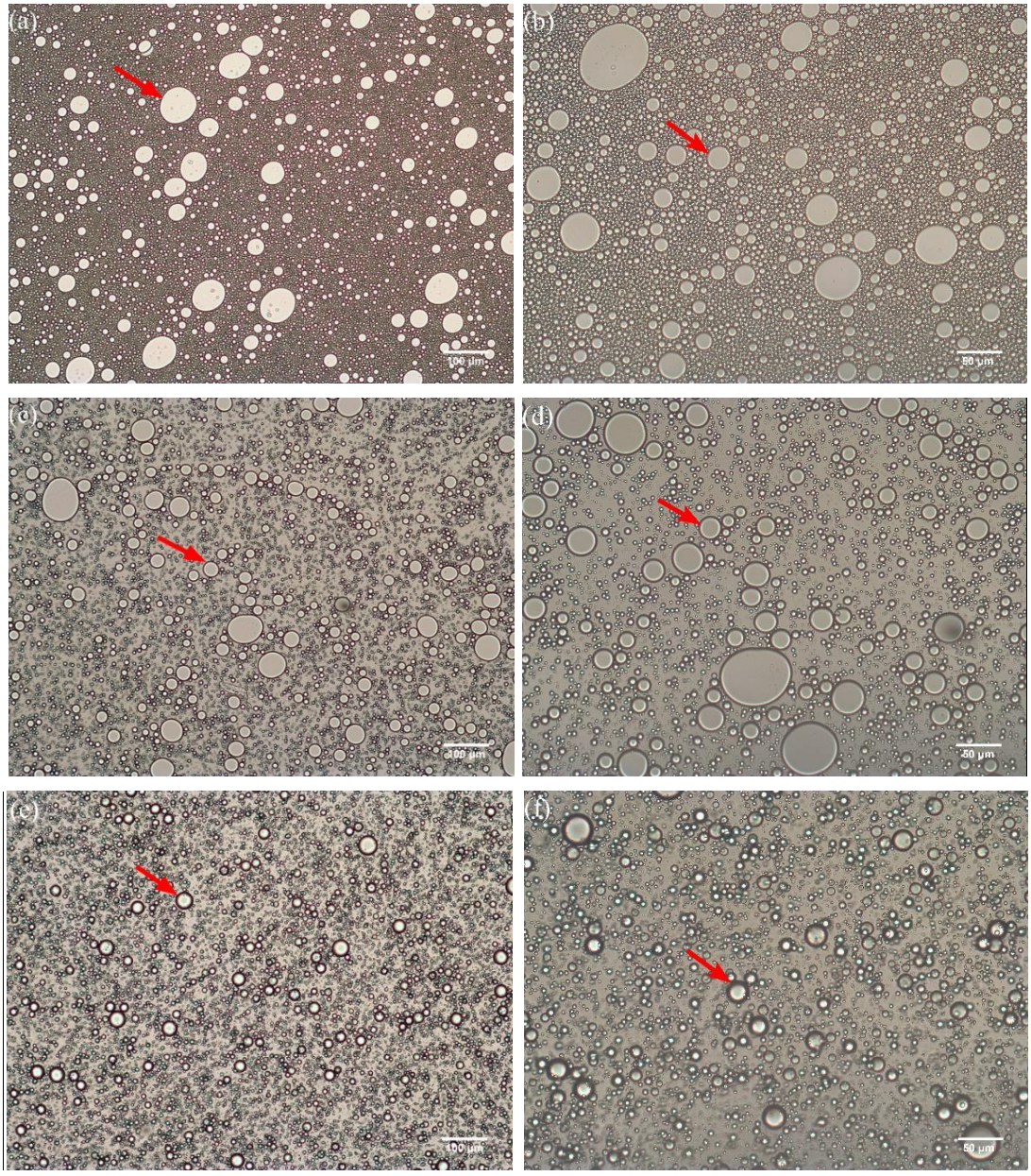

Figure 3.1: Optical microscopy images of PE samples were prepared at 1 wt% GL and (a, b) 0.6 wt% XG (sample I); (c, d) 1.4 wt% XG (sample II); (e, f) 1.6 wt% XG (sample III) concentrations. Scale bars: (a, c, e) 100 µm (10x); (b, d, f) 50 µm (20x).

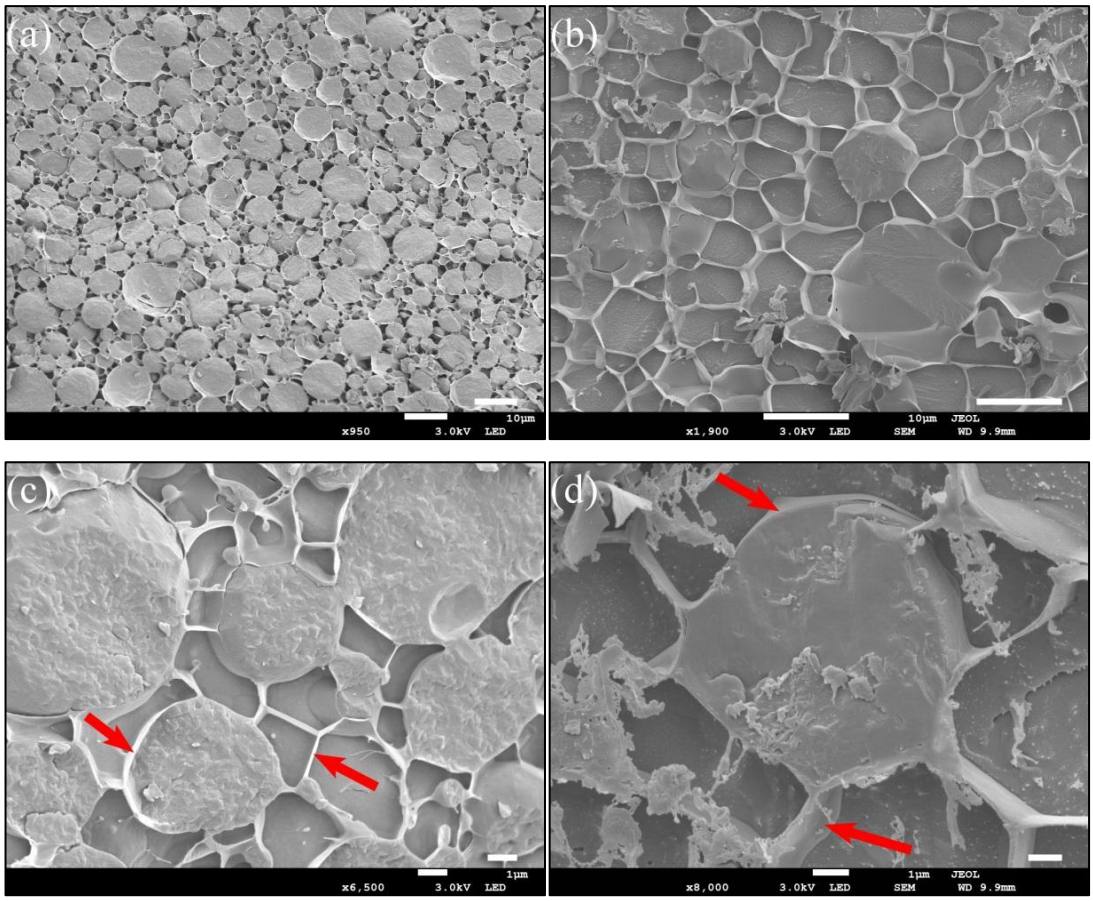

Figure 3.2: Cryogenic scanning electron microscopy images of PEs prepared by using sample I (a, c) at 0.6 wt% XG and sample II (b, d) at 1.4 wt% XG. Scale bars: (a) 10 µm; (b) 10 µm; (c) 1 µm and (d) 1 µm.

3.1.3 Particle size distribution of primary emulsion

The particle size distribution of an emulsion is an important quality parameter to be considered. Bimodal distribution indicates that (Figure 3.3) the emulsion is polydispersed in nature. Notice the way distribution curves shift to the right with the increase in XG concentration. The volume of the droplet size and maximum peak were higher at 1.6 wt% XG compared to 0.6 wt% and 1.4 wt% XG. Highest droplets sizes were 6.62 µm (at 6.42% volume) for 0.6 wt%, 10.48 µm (at 6.41% volume) for 1.4 wt%, 12.21 µm (at 6.65% volume) for 1.6 wt% respectively. Results showed that droplet size was increased by increasing XG ratio. It is important to note that for emulsions in which the concentration of XG was varied, the concentration of GL was kept constant at 1 wt%.

The volume weighted droplet size was also measured using Master Sizer (Figure 3.4). It was suggested that the volume weighted mean droplet size [$D_{4,3}$] for emulsion with 0.6 wt% XG (9.22 µm) was significantly lower than 1.4 wt% XG (17.21 µm)

and 1.6 wt% XG (16.89 µm). This result can be explained by the increase in viscosity of XG.

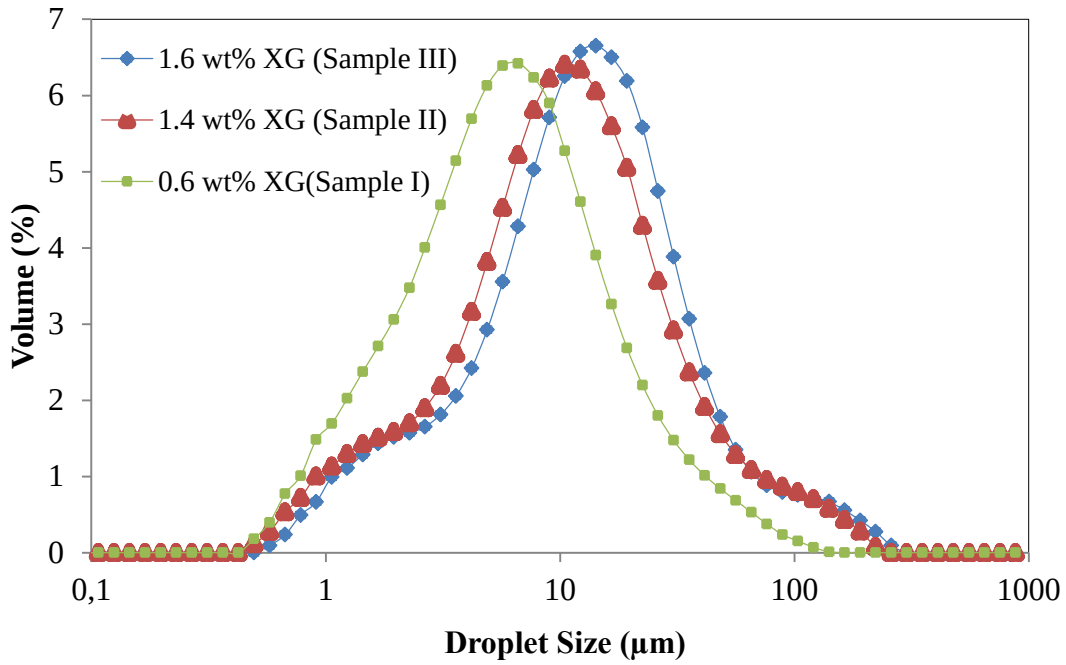

Figure 3.3: Droplet size distribution curves of PE samples prepared at 0.6 wt% XG (sample I); 1.4 wt% XG (sample II) and 1.6 wt% XG (sample III). Ultraturrax-type T 25B was used for emulsion preparation.

The result of particle size distribution was also confirmed by what was found in microscopic observation.

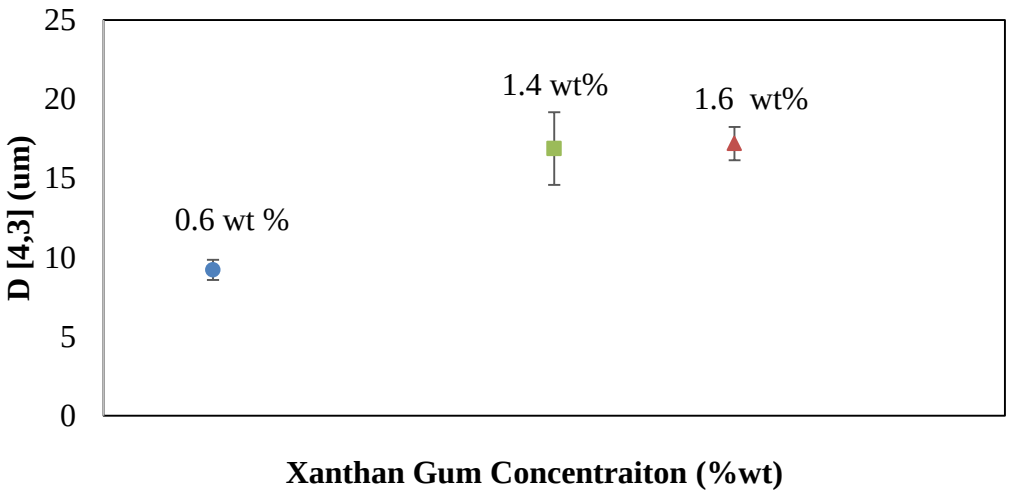

Figure 3.4: Volume-weighted mean droplet size, D[4,3] of PE samples prepared at 0.6 wt% XG (sample I); 1.4 wt% XG (sample II) and 1.6 wt% XG (sample III). Ultraturrax-type T 25B was used for emulsion preparation.

Droplets size results were done by Tukeys test showed in Table 3.1. According to table, changing XG concentration from 0.6 wt% to 1.6 wt% has significant effect on droplet size.

Table 3.1: Droplet sizes of PEs prepared at 0.6 wt% XG (sample I); 1.4 wt% XG (sample II); 1.6 wt% XG (sample III).

PE	Droplet Size (μm)
Sample I	9.22 ± 2.29^{a}
Sample II	17.21 ± 1.05^{bc}
Sample III	16.89 ± 0.63^{bc}

3.2 Characterization of Double Emulsions with Constant Water Concentration

3.2.1 Optical microscopy under normal light

Microstructure of O/W/O DEs under normal light, composed of 20 wt% water phase and 80 wt% fat phase in total was illustrated (Figure 3.5). Notice the water phase marked by arrows.

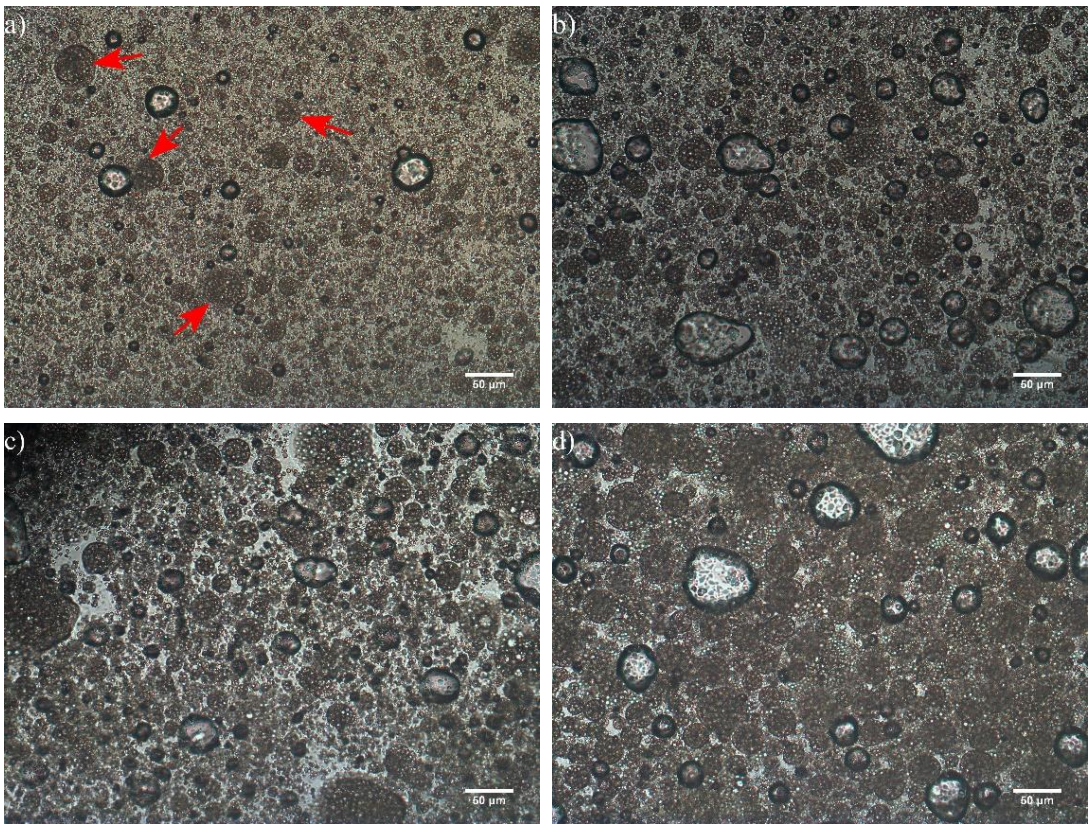

Figure 3.5: Normal light microscopy images of O/W/O DEs prepared at (a) 30 wt% SFO (sample IV); (b) 38.3 wt% SFO (sample V); (c) 46.7 wt% SFO (sample VI); (d) 55 wt% SFO (sample VII) concentrations. Scale bars: 50 μm (20x).

Clusters of droplets in the water phase were clearly visible and were indicated by red arrows in Figure 3.6a, as an example. In O_1/W phase, small SFO droplets were surrounded by a GL-XG blend. In W/O_2 phase, larger water droplets were surrounded by palm oil in an oil-continuous phase. It was assumed that there could be still some SFO that didn't encapsulate and stayed at the outer oil phase. Confocal microscope was further used to understand whether all SFOs were transferred to the internal water phase. Water phases were clearer on images on the right sides compared with the ones on the left sides as they were recorded at higher magnification. The results indicated that when SFO ratio increased from 30 wt% to 55 wt%, the internal water droplets became bigger which means that greater amount of SFO was encapsulated.

3.2.2 Optical microscopy under polarized light

Crystalline network formation of O/W/O DEs under polarized light microscopy (PLM) was illustrated in Figure 3.6.

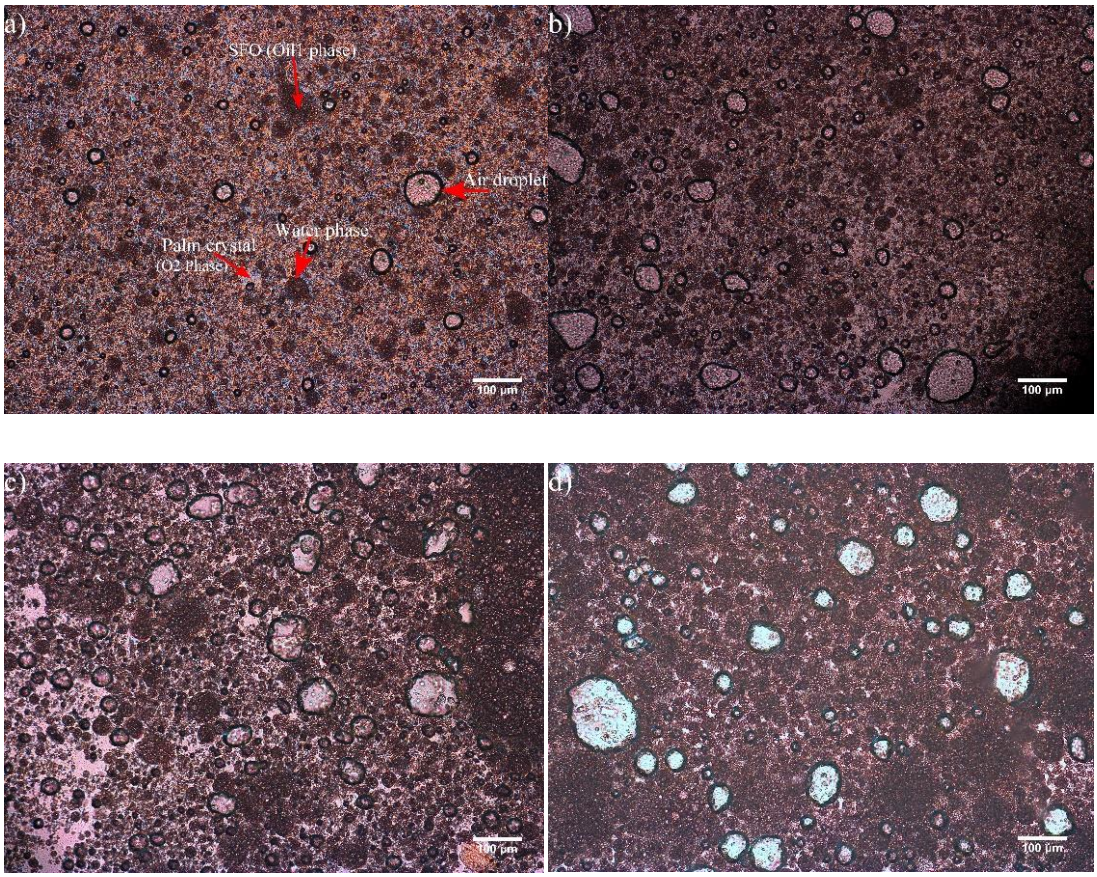

Figure 3.6: PLM images of O/W/O DEs prepared at (a) 30 wt% SFO (sample IV); (b) 38.3 wt% SFO (sample V); (c) 46.7 wt% SFO (sample VI); (d) 55 wt% SFO (sample VII) concentrations. Scale bars: 100 µm (10x).

Notice the water and oil phases marked by red arrows. All of O/W/O DEs were comprised of 20 wt% water phase and 80 wt% fat phase in total. As it was stated before, emulsions are made of water globules that contain small SFO droplets and this water phase dispersed in the second oil phase. Polarized light led us to see clearly blue fat crystals which represents the palm oil clearly. Although it was undesirable, there were also some air droplets (marked by the red arrow) with black layers. Air droplets were naturally formed during homogenisation by high-shear device and could be prevented with decreased movement of the cup used during shearing. The formation of fat crystal network in emulsions were less in the image d when compared with others. The reason for this is the decreasing proportion of palm oil from 50 wt% to 25 wt%.

3.2.3 Rhelogical behaviour

3.2.3.1 Linear viscoelastic region

The viscoelastic properties of emulsions are measured in an oscillation test. Oscillation is a technique in which a sinusoidal stress or strain is applied. Amplitude stress sweeps (stress = 0.1 to 3000 pa) were carried out to determine the linear viscoelastic region (LVR) of emulsions at a constant temperature rate of 20 ˚C /minute. The LVR was determined for each sample by varying concentration of SFO-palm oil. The storage modulus, G' (which indicates the gel stiffness) showed lower values for increasing SFO concentration (Figure 3.7). Shorter straight line with the increasing SFO concentration indicates that the network of emulsion stability weakened and the strength of emulsions decreased. 30 wt% SFO concentration was more stable with a straight line and had showed less variation between 1 and 100 pascal. However, for 60 wt% at lower stress (between 0.1-10 Pa) straight line was obtained. After 100 Pa, the emulsion was already broken meaning that it was not as strong as the others. The critical stress (a stress at which the LVR ends) decreased with the increasing SFO concentration, and this suggests that the proportion of SFO-palm oil has an impact on the rheology of the emulsion.

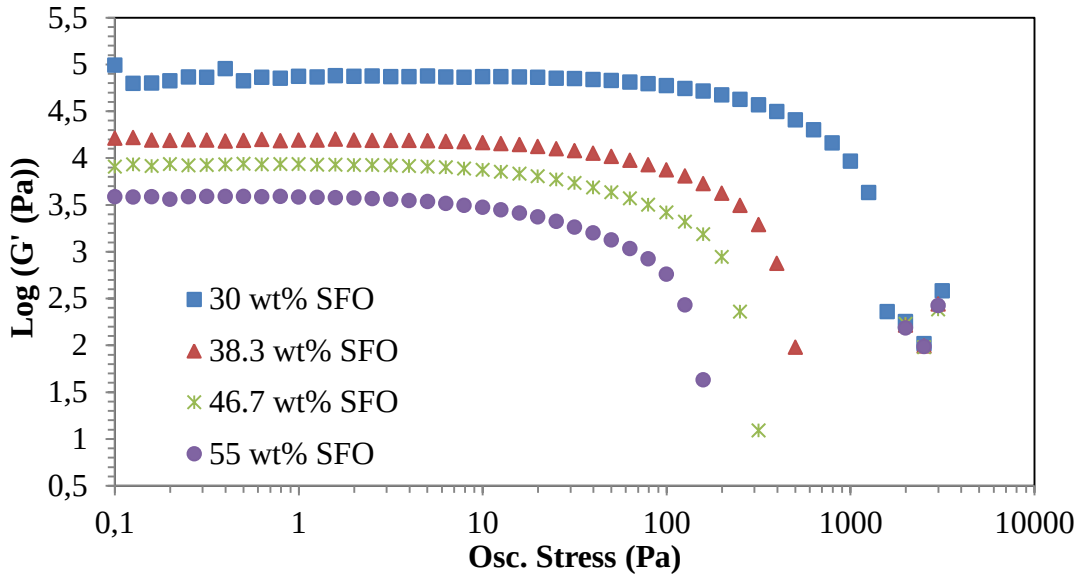

Figure 3.7: G' (Pa) plotted against oscillatory stress (Pa) for O/W/O DEs prepared at 30 wt% SFO (sample IV); 38.3 wt% SFO (sample V); 46.7 wt% SFO (sample VI) and 55 wt% SFO (sample VII) concentrations.

3.2.3.2 Frequency sweep

Frequency sweeps were carried out on emulsions samples at a oscillatory stress of 2 Pa (frequency of 0.1 to 100 Hz) and a constant temperature rate of 20 ˚C /minute. As seen in Figure 3.8, a slight positive slope in all cases indicates a weak gel structure of the emulsions. G' decreased proportionally with the increasing SFO concentration, which confirms that the increasing concentration of SFO against palm oil influences the gel stiffness of emulsions, one more time.

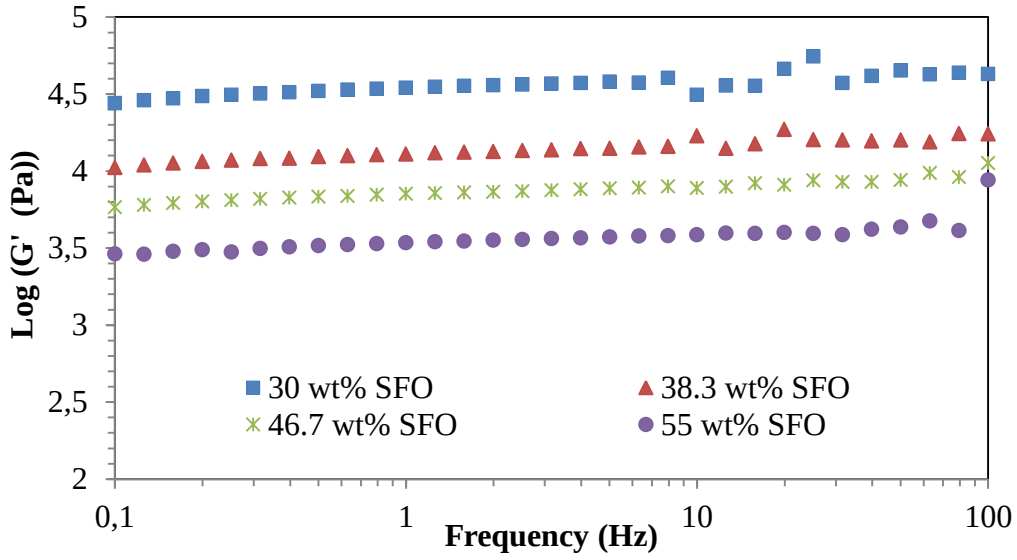

Figure 3.8: Frequency sweeps of O/W/O DEs at 30 wt% SFO (sample IV); 38.3 wt% SFO (sample V); 46.7 wt% SFO (sample VI) and 55 wt% SFO (sample VII) concentrations.

3.2.4 Texture analysis

Figure 3.9 shows the hardness of emulsions plotted as a function of SFO concentrations. The samples were stored overnight at 4 ˚C which were then characterized using large deformation fracture studies. The hardness results were compatible with rheological results. The hardness of the DEs decreased significantly with increasing SFO concentration which confirms that the proportion of SFO-palm oil had an observable effect on emulsion hardness.

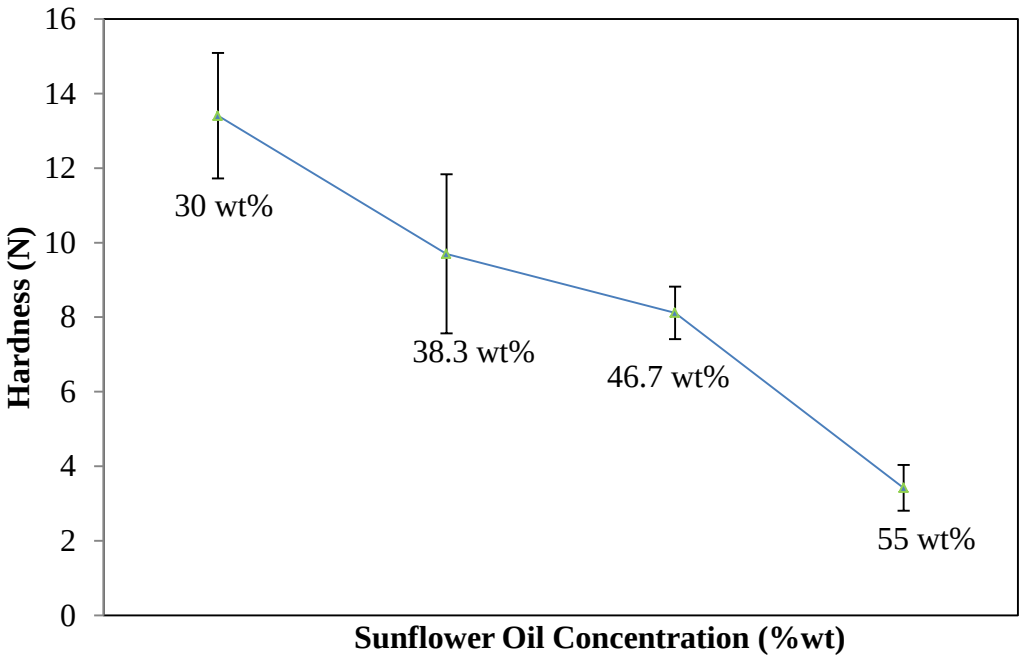

Figure 3.9: The effect of O/W/O DE concentrations at 30 wt% SFO (sample IV); 38.3 wt% SFO (sample V); 46.7 wt% SFO (sample VI) and 55 wt% SFO (sample VII) on the hardness.

Hardness results were done by Tukeys test showed in Table 3.2. According to table, changing SFO concentration from 30 wt% to 55 wt% has significant effect on hardness.

Table 3.2: Hardness values of DEs prepared at 30 wt% SFO (sample IV); 38.3 wt% SFO (sample V); 46.7 wt% SFO (sample VI) and 55 wt% SFO (sample VII) concentrations.

DE	Hardness (Newton)
Sample IV	13.40 ± 1.68^{a}
Sample V	9.70 ± 2.13^{bc}
Sample VI	8.12 ± 0.70^{bc}
Sample VII	3.42 ± 0.61^{d}

3.2.5 Thermal behaviour

DSC technique, based on the properties of solidification and melting of the droplets, is used to characterize O/W/O emulsions. The peak point of the recorded signal is called thermogram indicating the heat exchange during the thermal fact. The released energy during melting is an evidence of that the thermogram is endothermic (Dalmazzone et al, 2009). The thermogram obtained with heating in Figure 3.10 showed that solid palm starts to melt at 10 ˚C and completely melts at 40 ˚C and this is an important parameter to consider. The higher the SFO concentration showed the lower the peak area. Furthermore, the heat flow varied from one sample to another. From 0 ˚C to 20 ˚C, a significant amount of energy was released in a very short time. This is why the first part of the endothermic melting peak was sharp. The first endothermic peak corresponds to the eutectic melting of the emulsion followed by the second endothermic peak due to the progressive melting. The heat exchange was smaller and also decreased at higher SFO concentrations. Eutectic melting and the progressive melting represented palm oil and proved that total solidification occurred.

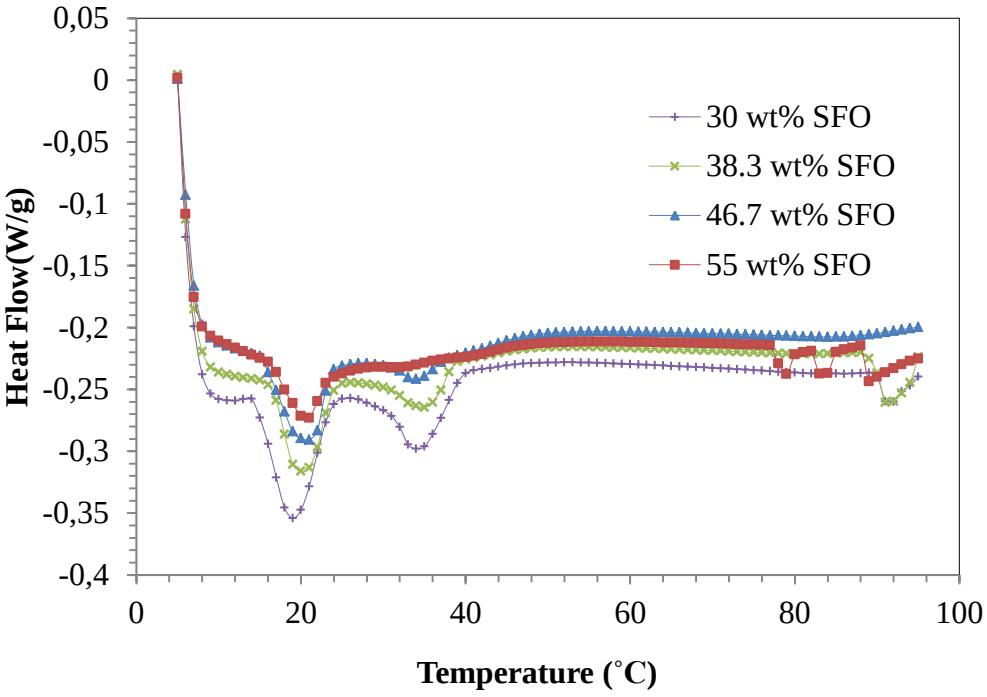

Figure 3.10: Heat flow (W/g) was plotted against temperature of O/W/O DEs at 30 wt% SFO (sample IV); 38.3 wt% SFO (sample V); 46.7 wt% SFO (sample VI) and 55 wt% SFO (sample VII) concentrations.

Thermal properties of DEs at different SFO concentrations presented in Table 3.3.

Table 3.3: Thermal properties of DEs prepared at 30 wt% SFO (sample IV); 38.3 wt% SFO (sample V); 46.7 wt% SFO (sample VI) and 55 wt% SFO (sample VII) concentrations.

DE	T_0 (˚C)	T_p (˚C)	T_e (˚C)	ΔH (J/g)
IV	14.23 ± 0.460 [a]	18.03 ± 0.714 [a]	22.73 ± 0.219 [a]	6.72 ± 0.72 [a]
V	17.23 ± 0.95 [a]	20.29 ± 0.78 [a]	23.71 ± 0.11 [b]	3.18 ± 1.28 [ab]
VI	16.59 ± 1.53 [a]	20.66 ± 0.47 [a]	23.47 ± 0.37 [ab]	3.19 ± 1.00 [ab]
VII	17.86 ± 1.63 [a]	20.53 ± 1.18 [a]	22.89 ± 0.01 [ab]	1.48 ± 1.19 [b]

3.2.6 Particle size distribution of double emulsion

The principle behind the droplet size analysis by pfg-NMR diffusometry relies on the comparison of the restricted diffusion of the water in the droplet to the free diffusing water.

Selection of diffusion time (Δ) depends on the largest droplet radius in the sample and the T_1-relaxation time of the water phase. Δ=0.36 second and Δ=0.66 second selected according to theoretical maximum accessible droplet radius. Average size and standard deviation of three repetition tubes are meausured. Using Δ=0.36 s, the estimated water droplet size distribution of the O/W/O emulsion is characterized by an average R_{43} of 8.91 ± 0.51 μm and average σ of 19.03 ± 1.26 μm. Using Δ=0.66 s, R_{43} and σ amounts to 10.23 ± 0.07 μm and 28.71 ± 2.58 μm, respectively (Table 3.4).

In comparison to Δ=0.36 second, the data obtained upon using Δ=0.66 second are characterized by larger estimate values and standard errors. The former might be due to an increase in extra droplet water diffusion with increasing Δ, whereas the latter follows from the decrease in residual signal with increasing Δ.

Table 3.4: Estimated water droplet size distribution of the 30/20/50 O/W/O emulsion (sample IV). The standard error of the estimation was included.

DE	Δ=0.36 second		Δ=0.66 second	
	R_{43} (μm)	σ (μm)	R_{43} (μm)	σ (μm)
Sample IV	8.91 ± 0.51	19.03 ± 1.26	10.23 ± 0.07	28.71 ± 2.58

3.3 Characterization of Double Emulsions with Different Water Concentrations

3.3.1 Double emulsions prepared from sample II

3.3.1.1 Optical microscopy under normal light

From the images, it is clearly seen that only with the help of XG and GL, DEs formed which contained 30, 40, 45 wt% water (Figure 3.11a,b,c). At 45 wt% water (c), 11.25 wt% SFO and 43.75 wt% palm oil were used. However, at 60 wt% water (d) SFO couldn't be transferred to the internal water droplets and no DE formation was observed because of the stability problem. This is the reason for adding 0.24 g PGPR as a surface active agent to melted palm oil to prepare 60 wt% water emulsion. And then, this mixture was homogenizated with PE. The results showed that even a small amount of PGPR can be useful to obtain DEs at 60 wt% water. It is important to note that at 60 wt% water SFO ratio was 15 wt% and palm oil ratio was low enough (25 wt%). As a result, to form DE at 60 wt% water, only 0.75 wt% GL, 1.05 wt%, XG and 0.4 wt% PGPR were used.

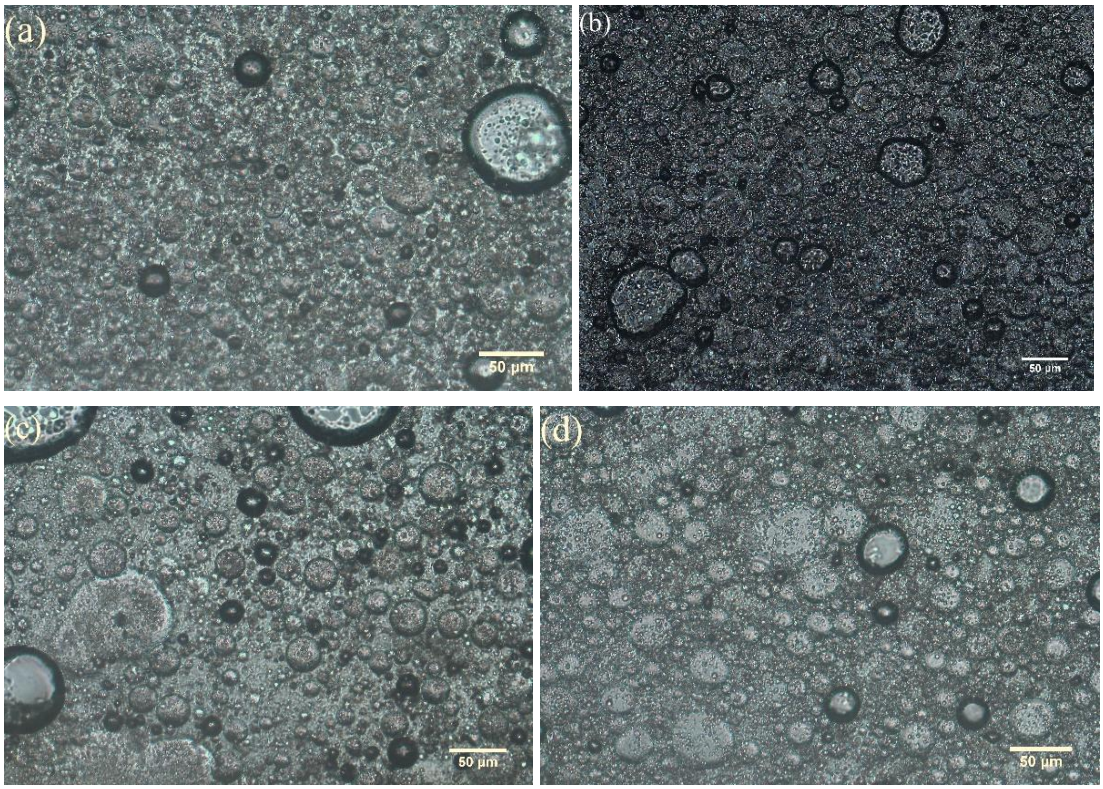

Figure 3.11: Optical microscopy images of O/W/O DEs (a) at 30 wt% water (sample VIII); (b) 40 wt% water (sample IX); (c) 45 wt% water (sample X); (d) 60 wt% water (sample XI) under normal light. Scale bars: 50 µm (20x).

3.3.1.2 Optical microscopy under polarized light

DEs were prepared with break and without break. Emulsion with two minutes break had better structure and there were more round droplets (Figure 3.12). This results indicates that continuous shear is not suitable for DE formation. As it was mentioned before DEs form at -0.15 ˚C. Continuous cooling could decrease emulsion's temperature lower than -0.15 ˚C. Two-minute break was given to keep temperature in the desired range.

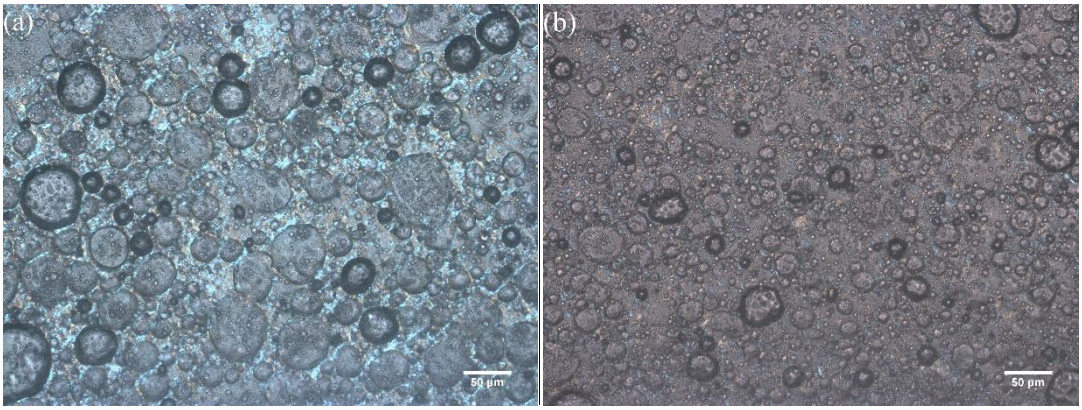

Figure 3.12: PLM images of 10/40/50 O/W/O DE (sample IX). Images represent (a) with 2-minute pause and (b) without any pause. Scale bars: 50 µm (20x).

As shown in the optical images in Figure 3.13, the stabilization of emulsion was a result of the interfacial crystallization. Blue fat crystals which were spread around water droplets equally, formed during cooling of the emulsion under continuous shear and prevented a coaleslence between droplets. The presence of fine crystallites at the interface confirms that when the used palm oil decreased from 62.5 wt% to 25 wt%, the amount of blue fat crystalls also decreased. In images a, b, d water droplets are almost completely round but on image c there are still some water droplets which are large and do not have a spherical shape. This can be explained by the unstability of DE as no emulsifier was used and can be solved by increasing the homogenization time. But it was observed that under 0 ˚C it is hard to catch the exact time as the form of DE can be broken easily. Also, the amount of water droplets were smaller at the 45 wt% water. This is because the formation of DE was going to be more difficult and the emulsion tried to convert a water continious phase when water ratio was increased. At 30 wt% water DEs had smaller droplet size as palm oil ratio higher which leads to more stable emulsions. At the 60 wt% water (Figure 3.13d) the

presence of PGPR ensures the dispersion of water into fine droplets, a crystallization occurs in the water–oil interfaces contributing to the stability of emulsion.

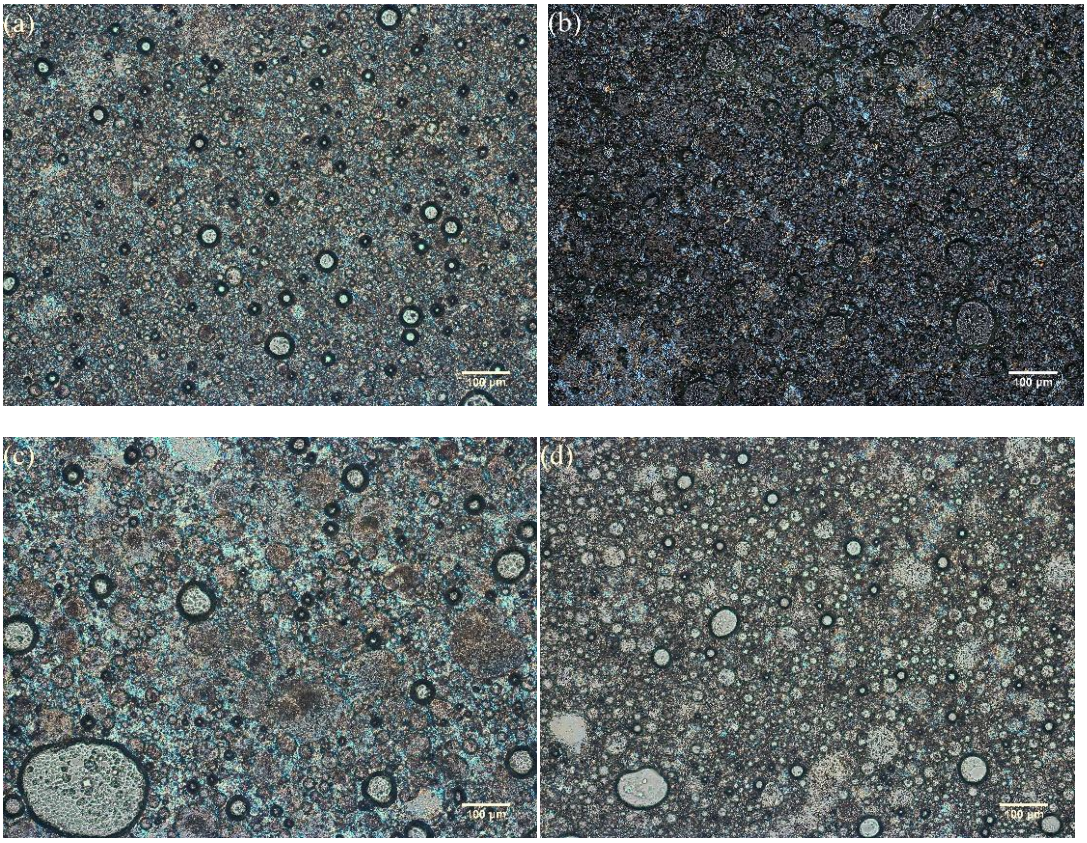

Figure 3.13 : Optical microscopy images of O/W/O DEs (a) at 30 wt% water (sample VIII); (b) 40 wt% water (sample IX); (c) 45 wt% water (sample X); (d) 60 wt% water (sample XI) under PLM. Scale bars: 100 μm (10x).

3.3.1.3 Optical microscopy after storage

As shown in Figure 3.14, the results were quite interesting: GL and XG were very efficient in encaptulation of SFO since DEs were still present. Additionally a significant effect of palm oil to prevent preventing stability should not be ignored. For 30 wt% water clear spherical shapes showed that the microstructure did not change very much after 7 days (Figure 3.14a,b). For 40 wt% water even on 60th day there were still quite a lot of internal water droplets (Figure 3.14c,d). For 45 wt% water on 14th day slight droplet deformation was observed and there was outer droplets coalescence in some parts (Figure 3.14e,f). The Amount of DEs decreased and they turned to a nonspherical shape. For 60 wt% water, the emulsion stability was already broken after 40 days. Images (g, h) confirm the coalescence and the disruption of the water phase.

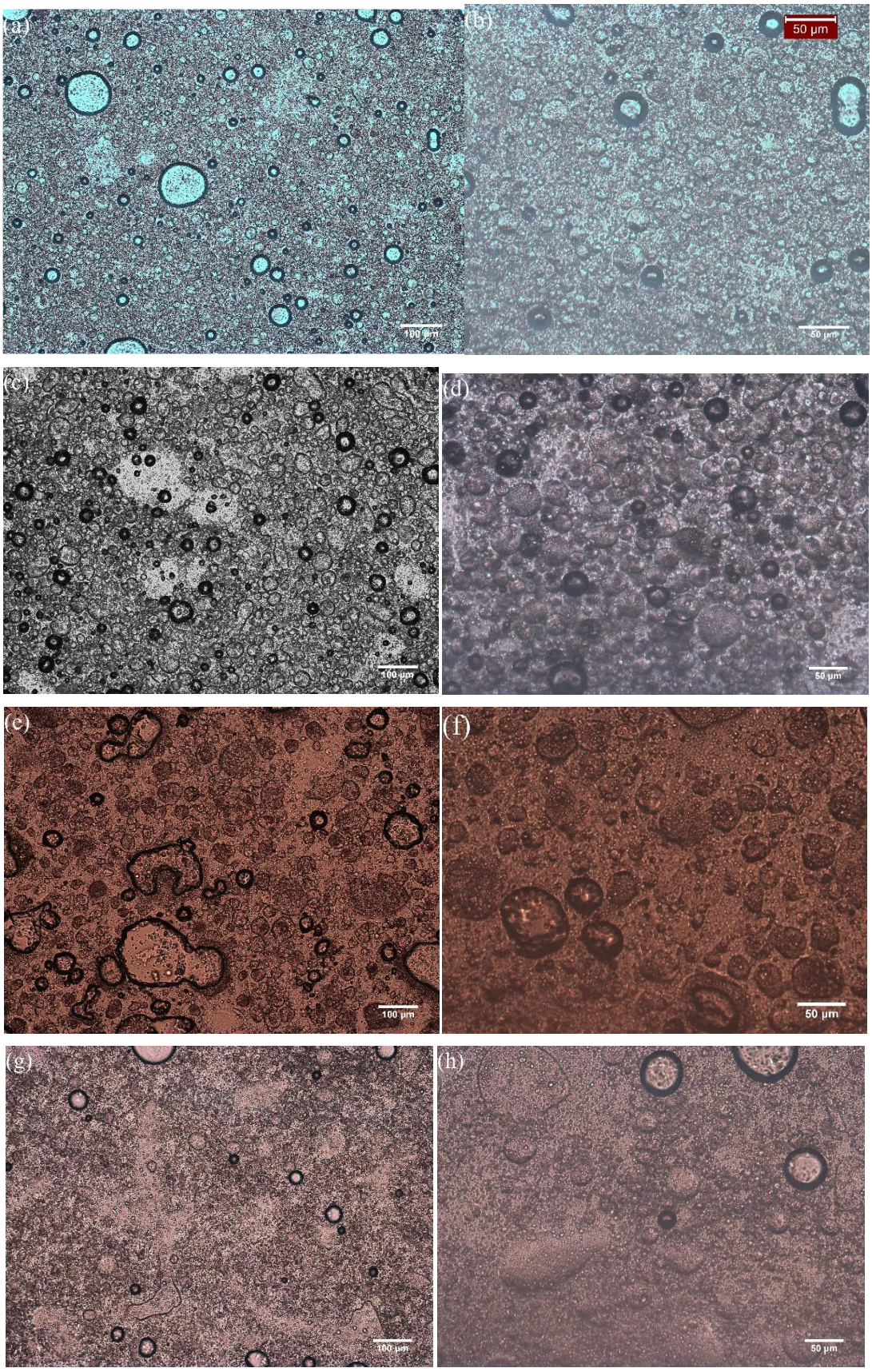

Figure 3.14: Optical microscopy images of O/W/O DEs after storage under normal light (a, b) at 30 wt% water (sample VIII); (c, d) 40 wt% water (sample IX); (e, f) 45 wt% water (sample X); (g, h) 60 wt% water (sample XI). Scale bars: (a, c, e, g) 100 µm (10x) and (b, d, f, h) 50 µm (20x).

After destabilisation of water phase, most of the SFO droplets were transferrred to the outer oil phase. However, there were still a few DEs left. All images showed that DEs were not distinct and not tightly packed together compered with the images before storage.

3.3.1.4 Cryogenic scanning electron microscopy

The Cryo-SEM images of freeze-fractured samples in Figure 3.15 confirms that the oil droplets do not have an internal contact, resembling the microstructure of a high-internal-phase emulsion. Images obtained after water removal. Figure 3.15a shows the spherical shapes that are hanging in the emulsion and images b, d and e the shows round structure that contains oil droplets (marked by arrows). The different form marked by the arrow in the middle can be explained by the working principle of Cryo-SEM, the removal of the upper layer caused to a hemispherically shape. From a clear angle (Figure 3.15b), the polymeric framework that was formed by surface-active polymer (GL) and non-surface active polymer (XG) in the bulk phase was clearer. The enlarged image of the oil droplet showed that Cryo-SEM structure can be recorded in very high magnifications compared with records of optical microscopy. On image (d), there were some black holes which represent air in the spherical shapes after the removal of dispersed water.

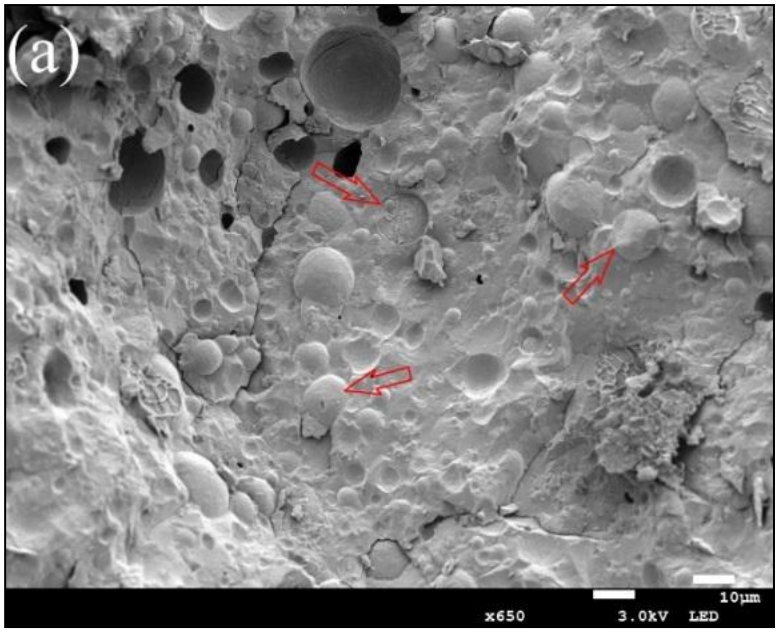

Figure 3.15: Cryogenic scanning electron microscopy images of emulsions (a, b) sample VIII; (c) sample IX; (d) sample X; (e) sample XI. inset: enlarged image of oil droplet showed the network of polymers around it (scale bar: 100 nm). Scale bars: (a, c, e) 10 µm and (b, d) 1 µm.

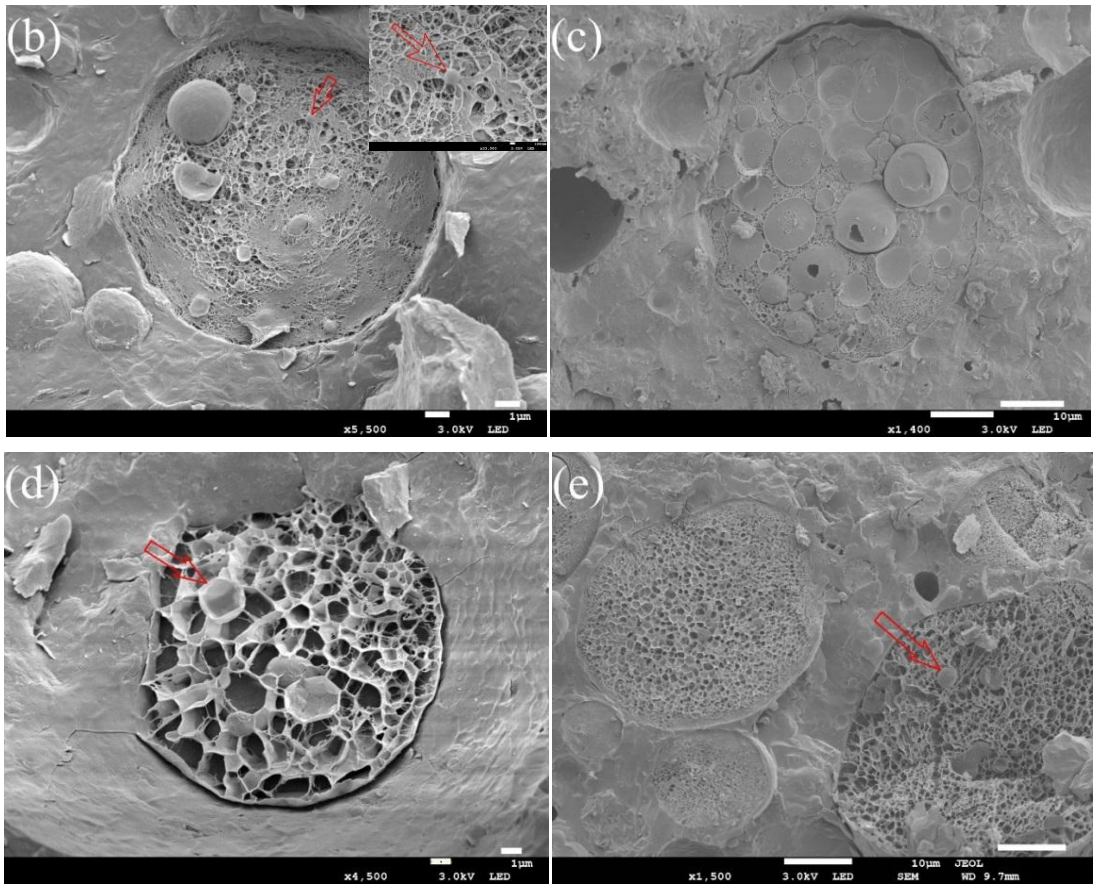

Figure 3.15 (continue): Cryogenic scanning electron microscopy images of emulsions (a, b) sample VIII; (c) sample IX; (d) sample X; (e) sample XI. inset: enlarged image of oil droplet showed the network of polymers around it (scale bar: 100 nm). Scale bars: (a, c, e) 10 μm and (b, d) 1 μm.

The presence of polymers at the interface and in the bulk phase confirmed that when the emulsions dried at high temperatures, the coalescence of the droplets were prevented. Image d contained 45 wt% water before removal that's why it had more air when compared with image c. On image e, also the presence of a solid SFO droplet (indicated by the red arrow) is clearly seen to be covered by well-formed interfaces.

3.3.1.5 Rhelogical behaviour

Amplitude sweeps (stress = 1 Pa−5000 Pa, frequency = 1 Hz) were carried out to define a linear viscoelastic region (LVR) of the DEs. In Figure 3.10, the thermal analysis results showed that the emulsion formation started to break after 10 ˚C. So, for rhelohical measurements analysis, the temperature was set to 10 ˚C this time. Comparable rheological properties in Figure 3.16 suggest that a short pause during homogenization has a positive effect on the length of the LVR.

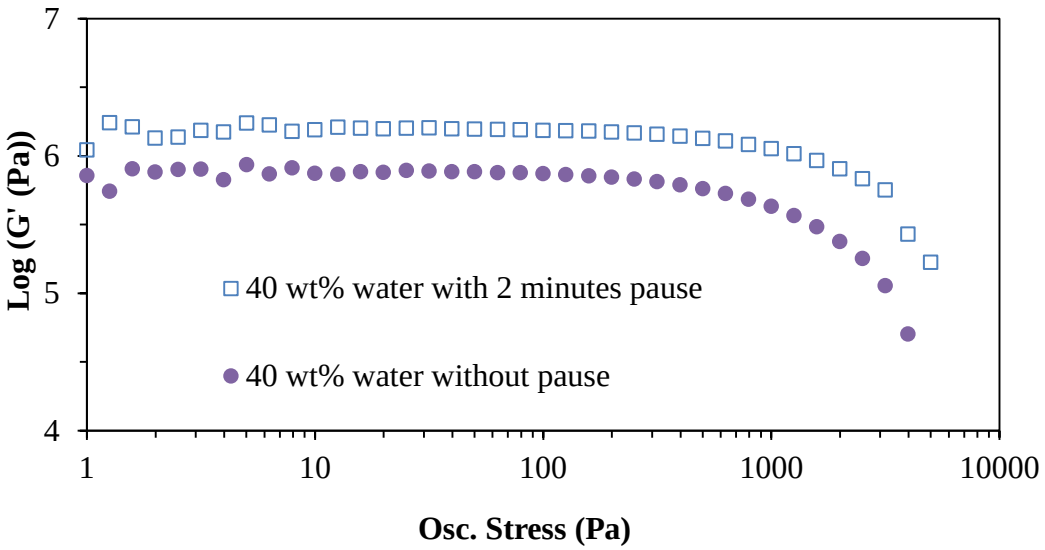

Figure 3.16: G' (Pa) plotted against oscillatory stress (Pa) for 10/40/50 O/W/O DE (sample IX) by giving a 2-minute pause and without any pauses.

The emulsion prepared without any break exhibited a lower viscosity value and lower critical oscillatory stress compared with the emulsion prepared with 2 minutes pause.

After deciding to give the break, amplitude sweeps were carried out to define the LVR of DEs. At 30 wt % water 0.1 Pa to 5000 Pa stress and 1 Hz frequency; at 40, 45 and 60 wt% water, 0.1 Pa to 3000 Pa stress and 1 Hz frequency was applied. The emulsions were compared in terms of their rheological properties and as expected, the increase in the water phase led to a decrease in the gel strength (Figure 3.17).

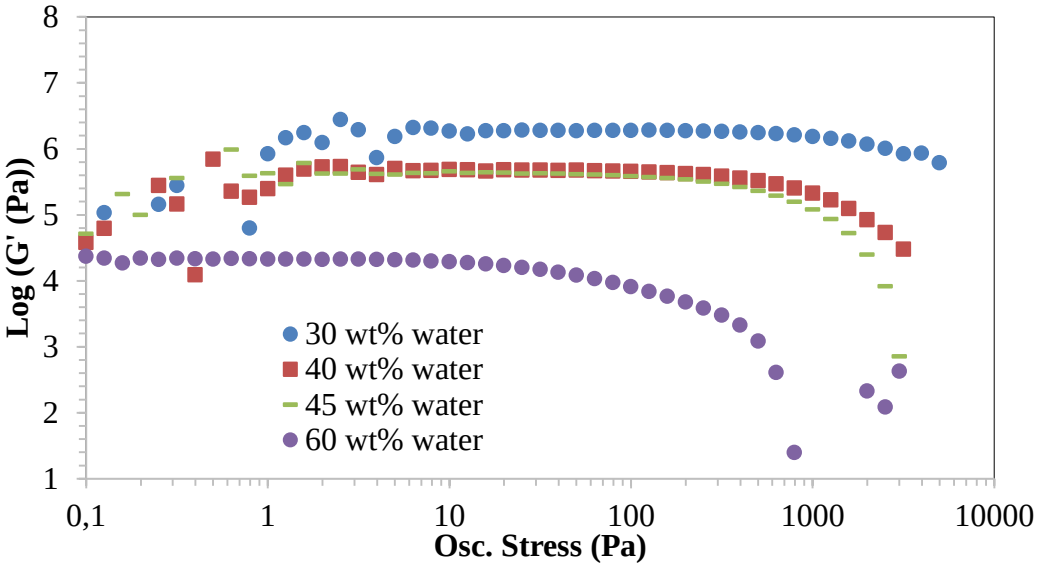

Figure 3.17 : G' (Pa) plotted against oscillatory stress (Pa) for O/W/O DEs prepared at 30 wt% water (sample VIII); 40 wt% water (sample IX); 45 wt% water (sample X); 60 wt% water (sample XI) concentrations.

The length of the LVR decreased with the increasing water concentration. Furthermore it is clear that LVR shifted to left with the increasing water concentration. At 30 wt%, the water emulsion still had a strong structure up to the stress of 5000 Pa. However, for the sample with 60 wt% water, the structure was already broken after 500 Pa.

The frequency sweeps were carried out on emulsions samples at an oscillatory stress of 25 Pa (30 wt% and 40 wt%), 20 Pa (45 wt%), and 3 Pa (60 wt%), with a frequency of 0.1 to 100 Hz and at 10 ˚C. The viscoelastic properties of the emulsions were compared through oscillatory frequency sweeps (Figure 3.18). As seen from the graph, a slightly positive slope of the curves in all cases suggests again a weak gel structure of the emulsions. The comparatively softer structure of the emulsion was clearly evident as G' was lower for 60% wt water as compared to 30 wt% water. G' decreased proportionally by the increasing water ratio which shows that the increasing concentration of the water influences the gel stiffness of the emulsions.

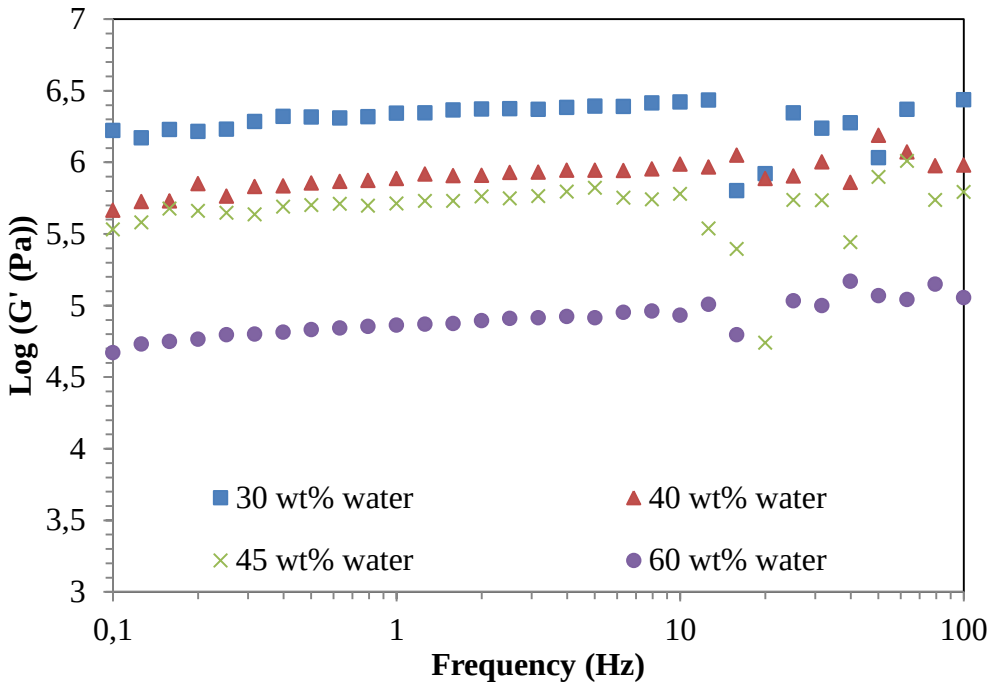

Figure 3.18: The frequency sweeps of O/W/O DEs at 30 wt% water (sample VIII); 40 wt% water (sample IX); 45 wt% water (sample X); 60 wt% water (sample XI) concentrations.

3.3.1.6 Texture anaylsis

Freshly prepared emulsion samples were stored overnight to get a gelled emulsion at a temperature around 5 ˚C. The texture analyzer was used to measure the hardness of

these gelled DEs. On varying levels of water concentration, a significant decrease in the hardness was observed especially for 60 wt% water (Figure 3.19). The increase in water concentration had a greater effect on the decrease of the hardness. The hardness indicating the gel stiffness showed higher values at 30 wt% water.

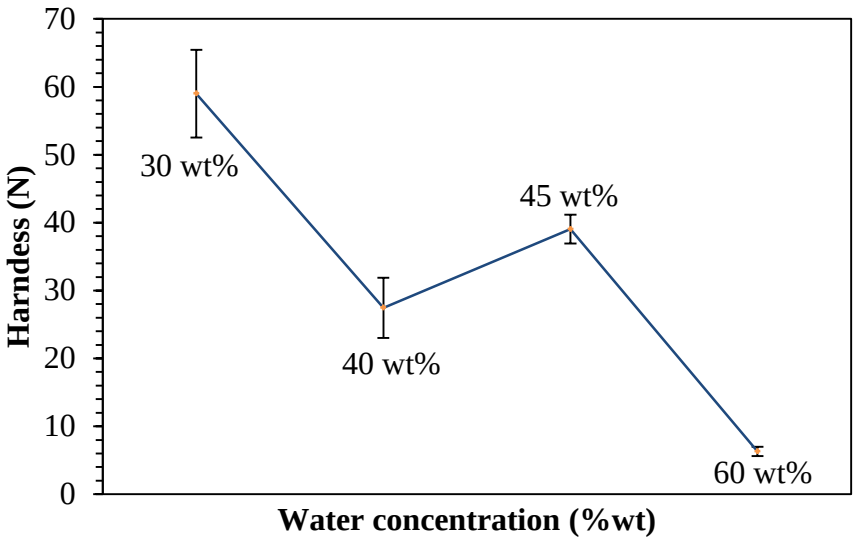

Figure 3.19: Hardness (N) plotted against at 30 wt% water (sample VIII); 40 wt% water (sample IX); 45 wt% water (sample X); 60 wt% water (sample XI) concentrations.

Hardness results were done by Tukeys test showed in Table 3.5. According to table, changing water concentration from 30 wt% to 60 wt% has significant effect on hardness.

Table 3.5: Hardness values of DEs prepared at 30 wt% water (sample VIII); 40 wt% water (sample IX); 45 wt% water (sample X); 60 wt% water (sample XI) concentrations.

DE	Hardness (Newton)
Sample VIII	58.99 ± 6.45^{a}
Sample IX	27.47 ± 4.43^{b}
Sample X	39.04 ± 2.13^{c}
Sample XI	6.32 ± 0.67^{d}

3.3.1.7 Thermal behaviour

In the DSC thermograms, the sample with 60 wt% water exhibited a single peak while multi-peak profiles were observed for the 30 wt%, 40 wt%, 45 wt% (Figure 3.20).

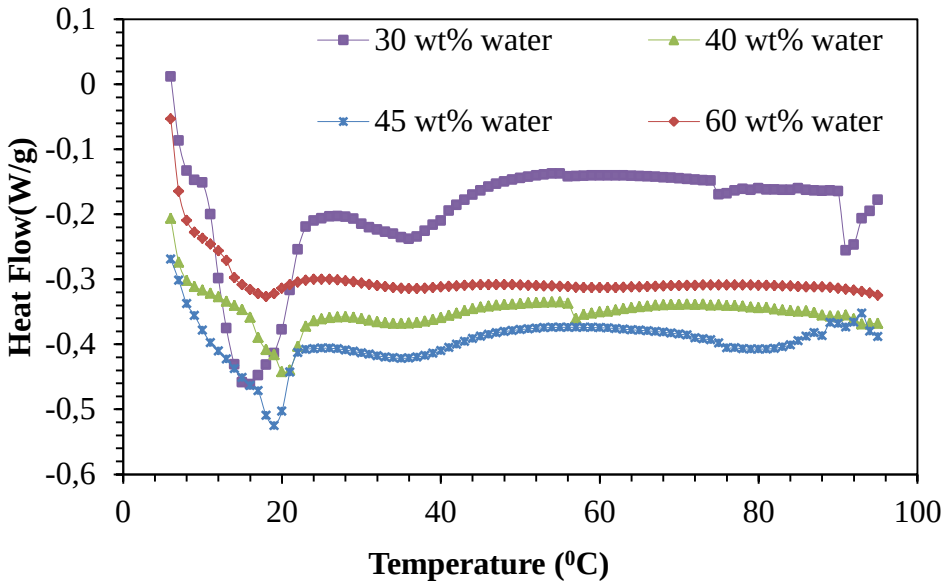

Figure 3.20: Heat flow (W/g) plotted agains temperature of O/W/O DEs at 30 wt% water (sample VIII); 40 wt% water (sample IX); 45 wt% water (sample X); 60 wt% water (sample XI) concentrations.

It was assumed that the first two peaks represent melting of the solid fat (palm oil). When the water was increased to the concentration of 40 wt%, the melting exotherm shifted to higher temperatures with two peaks. A steady heat flow was observed for the 60 wt% water after 20 ˚C, on the contrary for 30 wt% water, heat exchange was flexible and was the biggest one.

Thermal properties of DEs at different water concentrations presented in Table 3.6.

Table 3.6: Thermal properties of DEs prepared at 30 wt% water (sample VIII); 40 wt% water (sample IX); 45 wt% water (sample X); 60 wt% water (sample XI) concentrations.

DE	T_0 (˚C)	T_p (˚C)	T_e (˚C)	ΔH (J/g)
VIII	11.10 ± 0.16 ^{a}	15.41 ± 0.06 ^{a}	21.94 ± 0.12 ^{a}	20.52 ± 0.53 ^{a}
IX	17.65 ± 2.16 ^{a}	20.00 ± 1.39 ^{b}	22.59 ± 0.14 ^{a}	3.18 ± 2.42 ^{b}
X	15.79 ± 2.81 ^{a}	19.25 ± 0.66 ^{b}	21.33 ± 0.30 ^{ab}	3.38 ± 2.11 ^{b}
XI	12.85 ± 0.71 ^{a}	17.46. ± 0.42 ^{ab}	20.33 ± 0.59 ^{b}	1.89 ± 0.74 ^{b}

3.3.2 Double emulsions prepared from sample I

3.3.2.1 Optical microscopy under normal light

The microstructure of O/W/O DEs at 30/20/50 and 40/26.67/33.3 concentrations can be seen in Figure 3.21. DEs were bigger in shape but fewer in number when

compared with the previous ones. As SFO ratio increased to 30% wt and 40 % wt, more SFO was encapsulated and this resulted in bigger DEs. However, XG and GL ratio was lower and this probably has a negative impact on encapsulation efficieny and could cause the appearance of a greater amount of SFO in the outer oil phase.

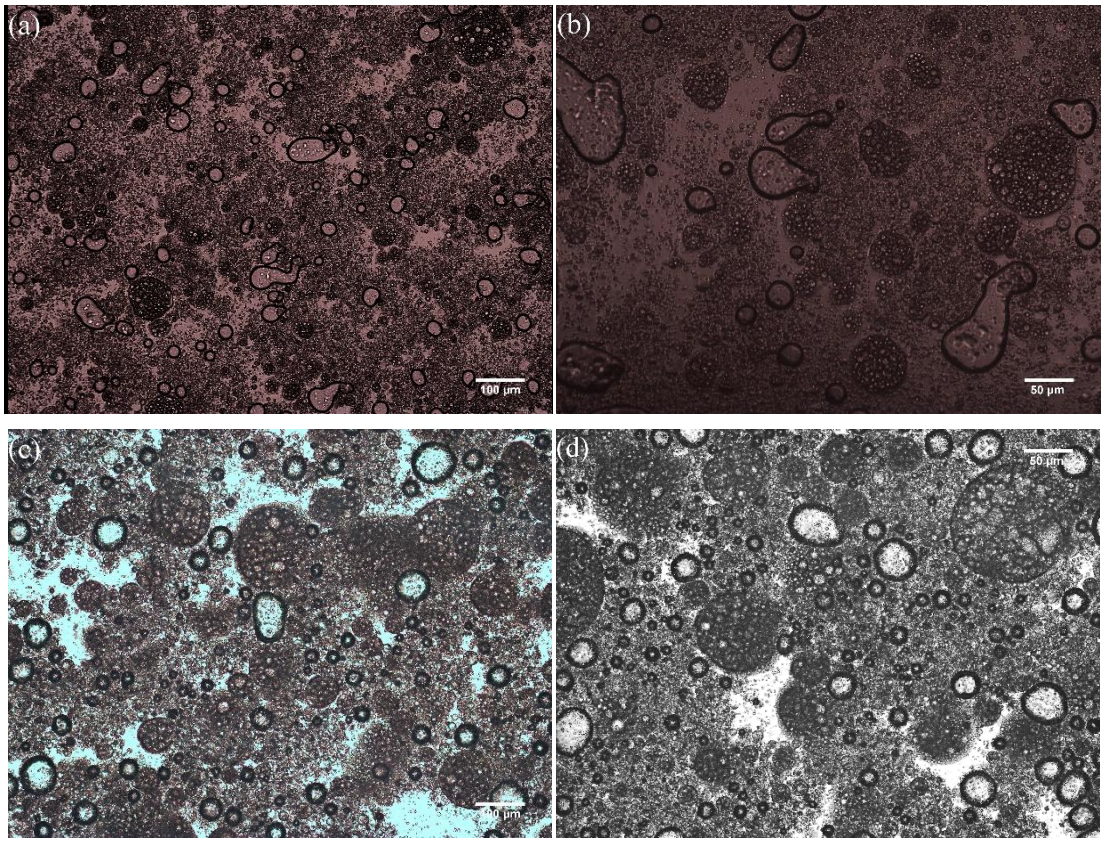

Figure 3.21: Normal light microscopy images of O/W/O DEs prepared at (a, b) 20 wt% water (sample XII); (c, d) 26.67 wt% water (sample XIII). Scale bars: (a, c) 100 µm (10x) and (b, d) 50 µm (20x).

3.3.2.2 Optical microscopy under normal light after storage

After 40 days of storage, the results were promising since DEs were still in a good shape. However, for the 30/20/50 emulsion (XII) some of the internal water droplets disappeared (Figure 3.22 a,b). For the 40/26.67/33.3 emulsion (XIII) as seen in Figure 3.22c and Figure 3.22d some internal water droplets were in close contact (marked by red arrows). This can be explained by insufficient barrier betweeen water phases when compared with the 30/20/50 emulsion because the palm oil ratio decreased to 33.3%.

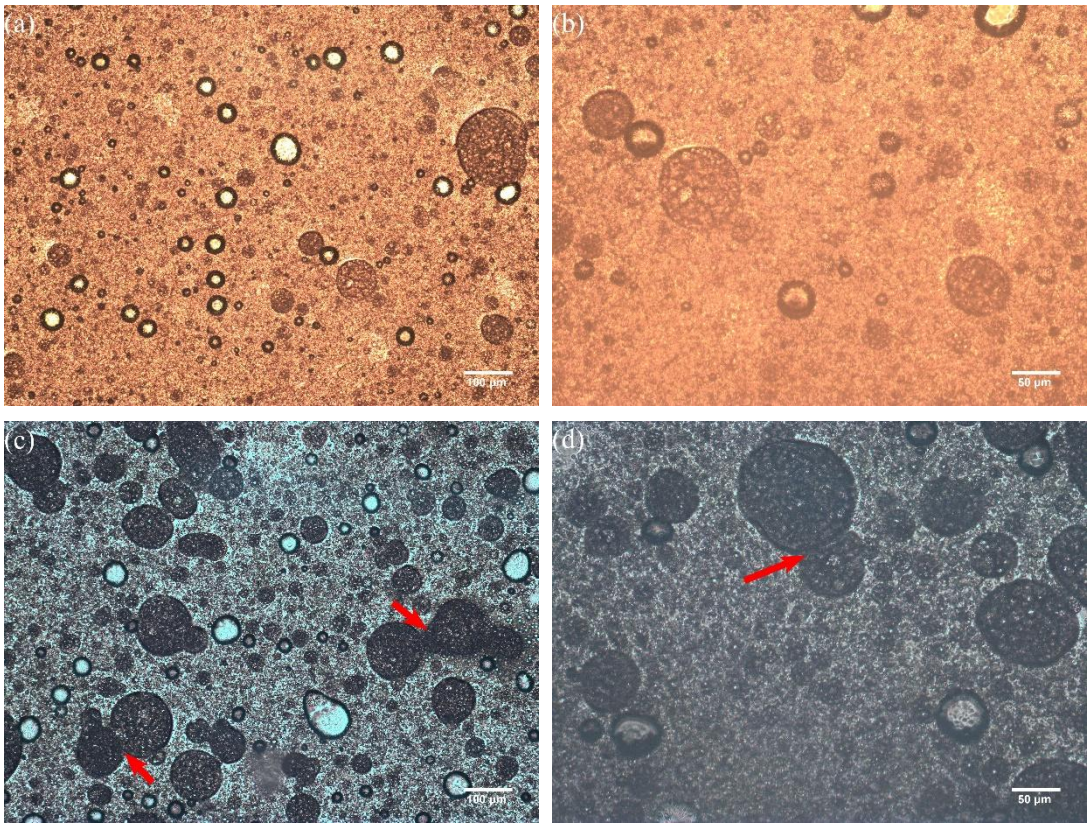

Figure 3.22: Normal light microscopy images of O/W/O DEs at 20 wt% water (a, b) (sample XII); 26.67 wt% water (c, d) (sample XIII) after 40 days of storage at 4 ^{0}C. Scale bars: (a, c) 100 µm (10x) and (b, d) 50 µm (20x).

3.3.2.3 Cryogenic scanning electron microscopy

In Figure 3.23a,b SFO droplets are more in amount when compared with previous Cry-SEM results as SFO ratio increased to 30 wt% and 40 wt% respectively.

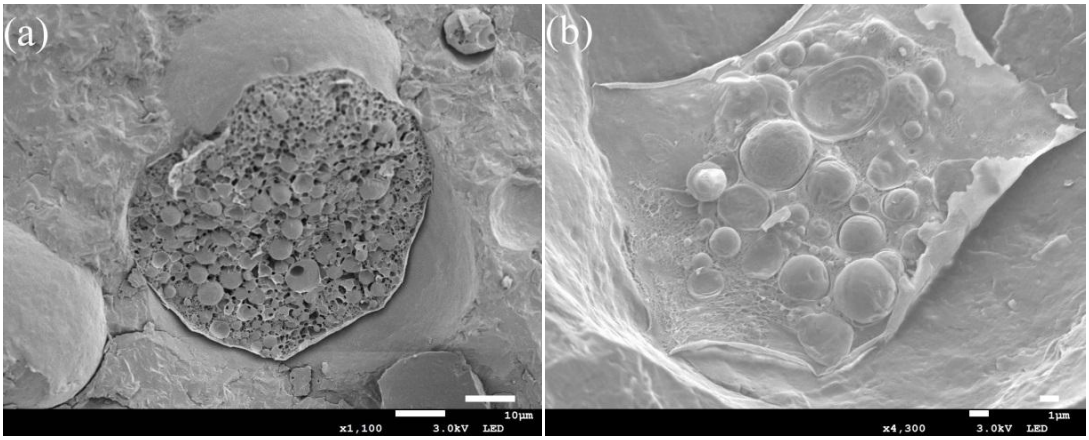

Figure 3.23: Cryogenic scanning electron microscopy images of emulsions prepared using 20wt% water (a) (sample XII) and 26.67 wt% water (b) (sample XIII). Images obtained after water removal. Scale bars: (a) 10 µm and (b) 1 µm.

However image at the right side does not have spherical shape. It is estimated that decreasing palm oil ratio to 33.3 wt% resulted in lower fat crystallization and prevented round shape formation.

3.3.2.4 Rheological behaviour

To determine the LVR, an amplitude sweeps (stress = 0.1 Pa−3000 Pa, frequency = 1 Hz) were performed. The results suggests that amount of water has an impact on the rheology of the emulsion (Figure 3.24). The increase in the concentration of water resulted in a decrease in the values of the G' as well as a decrease in the critical oscillatory stress. However, the LVR shifted to left at 26.67 %wt water.

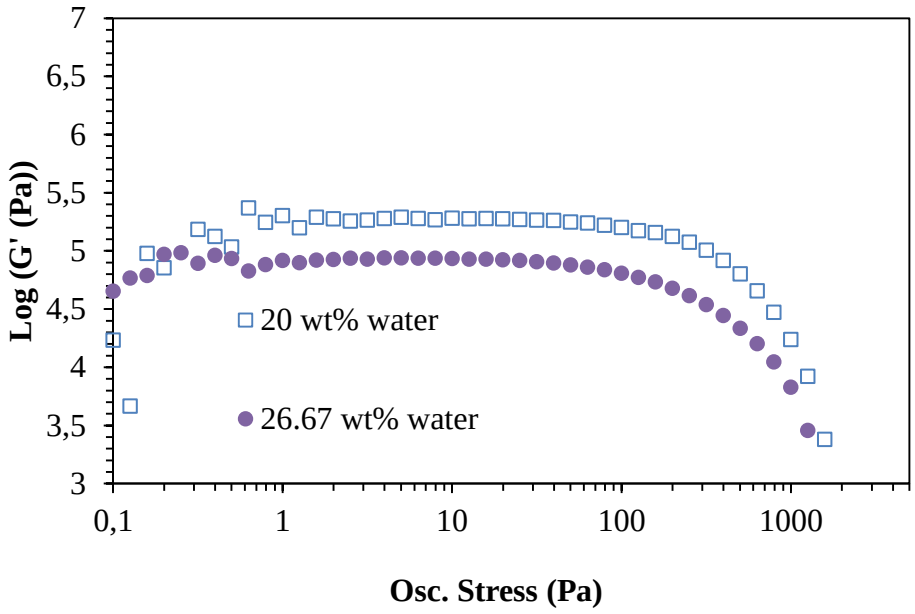

Figure 3.24: G' (Pa) plotted against oscillatory stress (Pa) for O/W/O DEs prepared at 20 wt% water (sample XII) and 26.67 wt% water (sample XIII) concentrations.

The dependence of the material response to the applied frequency was investigated by subjecting the samples to a stress of 10 Pa (20 wt% water) 6 Pa (26.67 wt% water) and that was within the region of linear response and frequencies from 0.1 to 100 Hz at 10 ˚C. The DEs rheological properties correspond to characteristic of a gel, shown in Figure 3.25. The graph shows a lower G' at 26.27 wt% water indicating that it has a softer structure, which is disrupted at a lower stress. The structure was broken after 10 Hz at 20 wt% water but there was not much deviation even up to 100 Hz at 26.27 wt% water comared with the other one. This result was in line with the results obtained from amplitude sweep stress and exhibited softer gel strength at 26.27 wt% water.

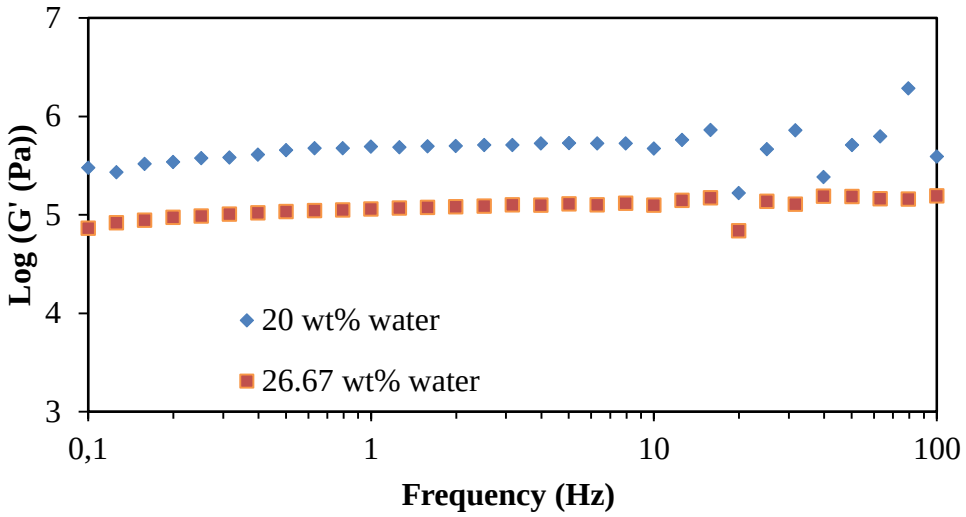

Figure 3.25: Frequency sweeps of O/W/O DEs at 20 wt% water (sample XII) and 26.67 wt% water (sample XIII) concentrations.

3.3.2.5 Texture analysis

The hardness data shown in Figure 3.26 indicates that the variation of water concentrations did not show major differences in the fracture properties of the samples ranging from 18.3 to 17.4 N. However, the samples hardness were lower when compared with the samples in Figure 3.20.

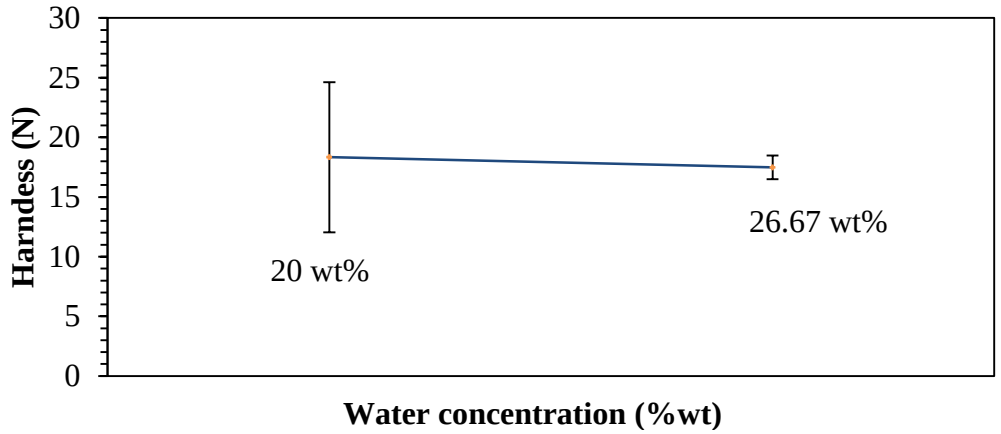

Figure 3.26: Hardness (N) plotted against at 20 wt% (sample XII) and 26.67 wt% (sample XIII) water concentrations of O/W/O DEs.

3.3.2.6 Thermal behaviour

Figure 3.27 shows the DSC thermogram for melting cycle of 20 wt% water and 26.67 wt% water. For sample at 26.67 wt% water, one peak was observed during this cycle, which appeared at a lower temperature.

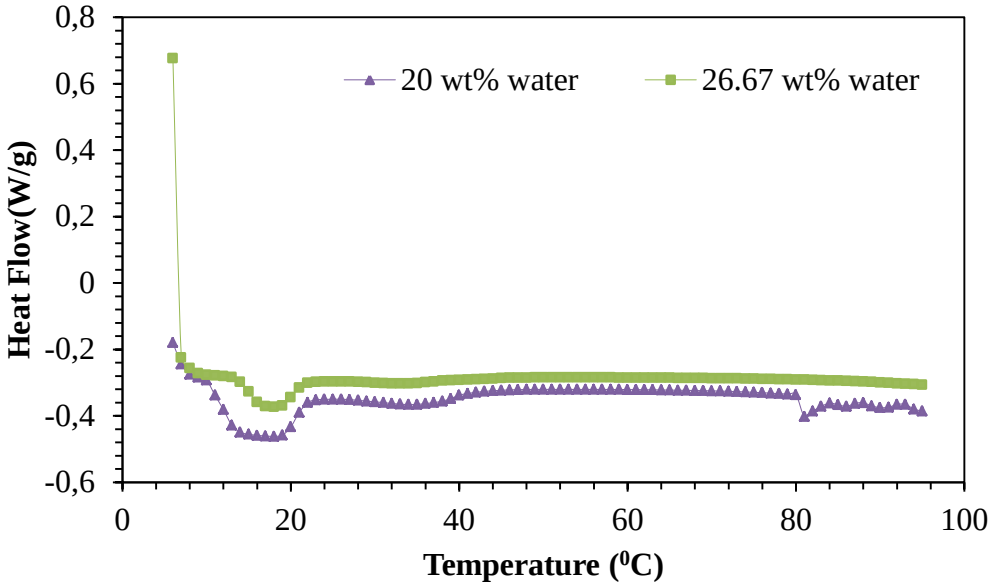

Figure 3.27: DSC spectrum of O/W/O DEs at 20 wt% water (sample XII) and 26.67 wt% water (sample XIII) concentrations plotted as heat flow (W/g) against temperature (^{0}C).

For sample at 20 wt% water, two peaks were observed and the second peak appeared at a higher temperature, the second one could also indicate the melting of the another fatty acid in the palm oil. At 20 wt% water, the samples have a larger range of heat flow between 5 ˚C and 10 ˚C but smaller heat flow between 10 ˚C and 20 ˚C when compared with other one.

Thermal properties of DEs at different water concentrations presented in Table 3.7.

Table 3.7: Thermal properties of DEs at 20 wt% water (sample XII) and 26.67 wt% water (sample XIII) concentrations.

DE	T_0 (˚C)	T_p (˚C)	T_e (˚C)	ΔH (J/g)
XII	10.93 ± 1.05	16.08 ± 2.65	21.68 ± 0.28	11.58 ± 4.33
XIII	14.36 ± 1.00	17.81 ± 0.68	21.19 ± 0.08	3.86 ± 1.21

3.4 Outcome

Main strategic purpose of utilization of O/W/O DEs in the present work was to encapsulate SFO with the help of biopolymers and to allow the production of the low-saturated fat products. A new way of creating and stabilizing O/W/O type of DE

in the presence of natural emulsifier (GL) and stabilizer (XG) was successfully achieved.

The core idea representing the formation of the oil-in-water-in-oil emulsion is illustrated in Figure 3.28. The red dots represent proteins whereas green strands represents polysaccharides.

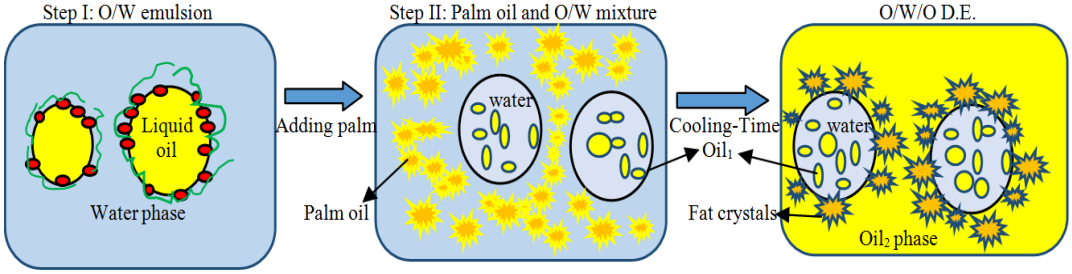

Figure 3.28: Schematic representations of homogenous mixed polysaccharide–protein emulsion (Step I), non homogenizous complex which contains hardstock (Step II), crystallization of fat crystalls by cooling and forming O/W/O DE.

PEs dispersed phase was structured using GL and XG. PEs were prepared succesfully with different water ratios and the structure of GL-XG based PEs were evaluated. The optical microscopy images confirmed the presence of polymer mixture around SFO droplets in water continuous emulsions and showed increase in XG from 0.6 wt% to 1.6 wt% at constant GL (1 wt%), which in turn resulted in an increase in DSD. The Cryo-SEM images of freeze-fractured samples suggested that the flocculated SFO droplets are surrounded by polymer network which provide a barrier and prevent the internal contact among the oil droplets. To obtain DEs, palm oil was added in PE to form the second oil phase which then formed fine water droplets. The DE formed with fat crystallization method by shearing mixture and it was subjected to a low temperature. Firstly, speed and time parameters were optimized for PE and DE. Then hard stock-water proportion was optimized and DEs were examined under the microscopes. The PLM images showed that droplets were surrounded by a mixture of solid fat spherulites and that a surface crystallization occurred. Increasing SFO from 35 wt% to 55 wt%, at the constant water content (20 wt%) in the presence of natural emulsifier gave promising results. Even at 55 wt% there were clear DEs. DEs were also obtained with an increasing water content from 30 wt% to 60 wt%. However, for 60 wt% water the stability of DE was preserved by inroducing a little amount of PGPR (0.4 %wt) which means palm oil ratio was reduced to 25 wt% in the outer oil phase. Finally, with the increasing amount of

water as well as the SFO content, DE with the O/W/O proportion of 40/26.67/33.3 was also obtained.

Thermal properties, DSD, rheological and textural properties were compared using DSC, pfg-NMR, Cryo-SEM to charactarize DE samples. The effect of different SFO ratios and different water ratios on the DEs texture were examined. The increased water ratio resulted in a decrease in hardness. Frequency sweep tests were applied and an amplitude sweep tests over a stress range was performed to determine the LVR. The DEs showed weak gel strength and an elastic bahavior. The results of the rheological anaylsis were compatible with the texture anaylsis results.

As a result of the experiments, it was assumed that DEs are formed in a very specific time and temperature range. Additionally, giving a short break during homogenization affected the rheological properties positively. The results were combined to optimize and formulate structured DEs as a template for oil structuring by transferring SFO in internal water droplets and reduced saturated fat applications.

The microstructure of DEs were recorded after long periods of time in storage for all samples and there were still DEs. The present microstructure of samples did not break until 60 days for the O/W/O ratio of 10/40/50. Yet, for the samples with the O/W/O ratio of 11.25/45/43.75, the stability was corrupted much more when compared with other DEs after 14 days.

The results of this research revealed that GL-XG mixture provided good O/W/O DE stability. The structuring of SFO resulted the interesting microstructure as the SFO droplets were transferred to the water phase where they tightly packed together in the polymer matrix. Furthermore, the crystallization of palm oil at the outer oil phase prevented the coalescence of water droplets. The results showed that liquid oil can transform into water droplets by using GL and XG with crysallization tenchnique and generating DEs with these biopolymers can be alternative to other synthethic emulsifiers.

4. CONCLUSIONS AND RECOMMENDATIONS

Hydrogenated oils such as palm oil, are high in saturated fats (~49.8 %) since they are used as hardstock for formulating emulsions. Palm oil has an important role in hidden fat contents in bakery products. However, saturated fats are considered unhealthy. On the other hand, there is a negative image associated with most surfactants because food manufacturers are looking for alternative approaches which could be used to reduce or eliminate emulsifiers in formulations based on complex colloidal systems. Accordingly, currently more detailed studies are ongoing to explore useful potentials of these DEs. The possibility of converting liquid oil into internal water droplets with the two step emulsification method could attract attention in food applications. It opens up the fascinating possibility in the food field with the less use of saturated fat, using natural and sustainable biopolymers. GL-XG combination can be used for producing of low-saturated fat products by transferring SFO into internal water droplets. As an alternavite to the previous methods the fat crystallization method is a promising technique for preparation of O/W/O DEs to encapsulate flavors. The DEs had an interesting microstructure wherein they were generated without the need for synthetic surface active agent. The interesting results of this research can lead in the developments of future studies on O/W/O DEs.

During the emulsification of the DEs the major problem was keeping temperature on the same level. Water bath could be used to overcome this matter when mixture subjected cooling. Furthermore, it was not clear whether all SFO droptlets transformed to water phase during emulsification. Confocal scanning laser microscopy was used to investigate whether all SFO was transferred to the internal water phase, however, this did not work. In the future studies, another fluorescent dye could be used instead of nile red for staining lipids while using microscopy in order to examine these.

O/W/O DEs may find potential applicatİon in flavor delivery applications for chocolates or bakery products. The promising results of these new types of DEs

warrant further studies: Encapsulation of flavors for flavor delivery applications or encapsulation of other compenents such as omega-3.

REFERENCES

Aserin, A. (Ed.). (2008). *Multiple emulsion: technology and applications* (Vol. 1). John Wiley & Sons.

Avendano-Gomez, J. R., Grossiord, J. L., & Clausse, D. (2005). Study of mass transfer in oil–water–oil multiple emulsions by differential scanning calorimetry. *Journal of colloid and interface science*, 290(2), 533-545.

Benichou, A., Aserin, A., & Garti, N. (2004). Double emulsions stabilized with hybrids of natural polymers for entrapment and slow release of active matters. *Advances in Colloid and Interface Science*, 108, 29-41.

Benichou, A., Aserin, A., & Garti, N. (2007). O/W/O double emulsions stabilized with WPI–polysaccharide conjugates. *Colloids and Surfaces A: Physicochemical and Engineering Aspects*, 297(1), 211-220.

Bernewitz, R., Schmidt, U. S., Schuchmann, H. P., & Guthausen, G. (2014). Structure of and diffusion in O/W/O double emulsions by CLSM and NMR–comparison with W/O/W. *Colloids and Surfaces A: Physicochemical and Engineering Aspects*, 458, 10-18.

Bouyer, E., Mekhloufi, G., Rosilio, V., Grossiord, J. L., & Agnely, F. (2012). Proteins, polysaccharides, and their complexes used as stabilizers for emulsions: alternatives to synthetic surfactants in the pharmaceutical field. *International journal of pharmaceutics*, 436(1), 359-378.

Cho, Y. H., & Park, J. (2003). Evaluation of process parameters in the O/W/O multiple emulsion method for flavor encapsulation. *Journal of food science*, 68(2), 534-538.

Clausse, D., Gomez, F., Pezron, I., Komunjer, L., & Dalmazzone, C. (2005). Morphology characterization of emulsions by differential scanning calorimetry. *Advances in Colloid and Interface Science*, 117(1), 59-74.

Dalmazzone, C., Noïk, C., & Clausse, D. (2009). Application of DSC for emulsified system characterization. Oil & Gas Science and Technology-Revue de l'IFP, 64(5), 543-555.

Davis, S. S., & Walker, I. M. (1987). Multiple emulsions as targetable delivery systems. *Methods in enzymology*, 149, 51.

Dickinson, E. (2011). Double emulsions stabilized by food biopolymers. *Food Biophysics*, 6(1), 1-11.

Dickinson, E., & Euston, S. R. (1991). *Stability of food emulsions containing both protein and polysaccharide* (pp. 132-146). Royal Society of Chemistry: Cambridge, UK.

Edris, A., & Bergnståhl, B. (2001). Encapsulation of orange oil in a spray dried double emulsion. *Food/Nahrung*, *45*(2), 133-137.

Frank, K., Köhler, K., & Schuchmann, H. P. (2011). Formulation of labile hydrophilic ingredients in multiple emulsions: influence of the formulation's composition on the emulsion's stability and on the stability of entrapped bioactives. *Journal of Dispersion Science and Technology*, *32*(12), 1753-1758.

Hee, L. L. Y., Jacquot, M., Hardy, J., & Desobry, S. (2008). Formulating polymeric gels simulating soft cheeses' texture. *Food hydrocolloids, 22*(5), 925-933.

Imeson, A. (Ed.). (2011). *Food stabilisers, thickeners and gelling agents.* John Wiley & Sons.

Jahaniaval, F., Kakuda, Y., & Abraham, V. (2003). Characterization of a double emulsion system (oil-in-water-in-oil emulsion) with low solid fats: Microstructure. *Journal of the American Oil Chemists' Society, 80*(1), 25-31.

Kumar, A. D. (2011). *Evaluation of selected matrix material for developing emulsion based delivery systemfor Pueraria tuberose/Vidarikand extract.* Masters in Technology thesis in Dairy Technology submitted to National Dairy Research Institute (Deemed University). Karnal, Haryana: India.

Kumar, R. A. J. E. S. H., Kumar, M. S., & Mahadevan, N. A. N. J. A. I. A. N. (2012). Multiple emulsions: a review. *International Journal of Recent Advances in Pharmaceutical Research, 2*(1), 9-19.

Lam, R. S., & Nickerson, M. T. (2013). Food proteins: a review on their emulsifying properties using a structure–function approach. *Food chemistry*, *141*(2), 975-984.

Lamba, H., Sathish, K., & Sabikhi, L. (2015). Double emulsions: Emerging delivery system for plant bioactives. *Food and Bioprocess Technology*, *8*(4), 709-728.

Li, B., Jiang, Y., Liu, F., Chai, Z., Li, Y., Li, Y., & Leng, X. (2012). Synergistic effects of whey protein–polysaccharide complexes on the controlled release of lipid-soluble and water-soluble vitamins in W1/O/W2 double emulsion systems. *International Journal of Food Science & Technology*, *47*(2), 248-254.

Liao, L., Luo, Y., Zhao, M., & Wang, Q. (2012). Preparation and characterization of succinic acid deamidated wheat gluten microspheres for encapsulation of fish oil. *Colloids and Surfaces B: Biointerfaces, 92*, 305-314.

Lii, C. Y., Liaw, S. C., Lai, V. F., & Tomasik, P. (2002). Xanthan gum–gelatin complexes. *European Polymer Journal*, *38*(7), 1377-1381.

Lin, S. W. (2002). Palm oil. *Vegetable oils in food technology: Composition, properties and uses*, 59.

List, G. R., Kritchevsky, D., & Ratnayake, W. M. (2007). *Trans fats in foods.* AOCS Press.

Lutz, R., Aserin, A., Wicker, L., & Garti, N. (2009). Release of electrolytes from W/O/W double emulsions stabilized by a soluble complex of modified pectin and whey protein isolate. *Colloids and Surfaces B: Biointerfaces, 74*(1), 178-185.

ABasic Guide to ParticleCharacterazation. Malvern Instruments. (2012). Retrieve fromhttp://golik.co.il/Data/ABasicGuidtoParticle Characterization(2)_1962085150.pdf. Accessed 05 April 2014.

Marangoni, A. G., & Garti, N. (2011). An overview of the past, present and future of organogels. *Edible oleogels: Structure and health implications*, 1-17.

Murday, J. S., & Cotts, R. M. (1968). Original mathematical solution for NMR data produced by identical spherical isolated droplets. *Journal of Chemical Physics*, 48, 4938-4945.

Muschiolik, G., & Bunjes, H. (Eds.). (2007). *Multiple Emulsionen: Herstellung und Eigenschaften.* Behr's Verlag DE.

O'Regan, J., & Mulvihill, D. M. (2009). Water soluble inner aqueous phase markers as indicators of the encapsulation properties of water-in-oil-in-water emulsions stabilized with sodium caseinate. *Food Hydrocolloids, 23*(8), 2339-2345.

O'Dwyer, S. P., O'Beirne, D., Eidhin, D. N., Hennessy, A. A., & O'Kennedy, B. T. (2013). Formation, rheology and susceptibility to lipid oxidation of multiple emulsions (O/W/O) in table spreads containing omega-3 rich oils. *LWT-Food Science and Technology, 51*(2), 484-491.

Patel, A. R., Rajarethinem, P. S., Cludts, N., Lewille, B., De Vos, W. H., Lesaffer, A., & Dewettinck, K. (2014). Biopolymer-based structuring of liquid oil into soft solids and oleogels using water-continuous emulsions as templates. *Langmuir, 31*(7), 2065-2073.

Patel, A. R., & Dewettinck, K. (2015). Current update on the influence of minor lipid components, shear and presence of interfaces on fat crystallization. *Current Opinion in Food Science*, 3, 65-70.

Patino, J. M. R., & Pilosof, A. M. (2011). Protein–polysaccharide interactions at fluid interfaces. *Food Hydrocolloids, 25*(8), 1925-1937.

Poku, K. (2002). *Small-scale palm oil processing in Africa* (Vol. 148). Food & Agriculture Org.

Pradhan, M., & Rousseau, D. (2012). A one-step process for oil-in-water-in-oil double emulsion formation using a single surfactant. *Journal of colloid and interface science, 386(*1), 398-404.

Prakash, W. V. (2012). *Studies on design of micro/nano emulsion based delivery system for potential nutraceuticals using dairy-based ingredients.* Masters in Technology thesis in Dairy Technology submitted to National Dairy Research Institute (Deemed University), Karnal, Haryana, India.

Sajjadi, S., Jahanzad, F., & Brooks, B. W. (2002). Phase inversion in abnormal O/W/O emulsions: I. Effect of surfactant concentration. *Industrial & engineering chemistry research, 41*(24), 6033-6041.

Sapei, L., Naqvi, M. A., & Rousseau, D. (2012). Stability and release properties of double emulsions for food applications. *Food hydrocolloids, 27*(2), 316-323.

Schmitt, C., Sanchez, C., Desobry-Banon, S., & Hardy, J. (1998). Structure and technofunctional properties of protein-polysaccharide complexes: a review. *Critical Reviews in Food Science and Nutrition*, 38(8), 689-753.

Steffe, J. F. (1996). *Rheological Methods in Food Process Engineering*, second edition (second printing). Freeman Press, East Lansing, MI, USA, 428p.

Van Duynhoven, J. P. M., Goudappel, G. J. W., Van Dalen, G., Van Bruggen, P. C., Blonk, J. C. G., & Eijkelenboom, A. P. A. M. (2002). Scope of droplet size measurements in food emulsions by pulsed field gradient NMR at low field. *Magnetic Resonance in Chemistry, 40*(13), S51-S59.

VAN Lent, K., Vanlenberghe, B., Van Oostveldt, P., Thas, O., & Van Der Meeren, P. (2008). Determination of water droplet size distribution in butter: Pulsed field gradient NMR in comparison with confocal scanning laser microscopy. *International dairy journal, 18*(1), 12-22.

Wang, S., Chen, Y., Liang, H., Chen, Y., Shi, M., Wu, J., ... Li, Y. (2015). Intestine-specific delivery of hydrophobic bioactives from oxidized starch microspheres with an enhanced stability. *Journal of agricultural and food chemistry, 63*(39), 8669-8675.

Wilde, P., Mackie, A., Husband, F., Gunning, P., & Morris, V. (2004). Proteins and emulsifiers at liquid interfaces. *Advances in Colloid and Interface Science, 108*, 63-71.

APPENDICES

APPENDIX A: Droplet size values

APPENDIX B: Hardness values

APPENDIX C: Thermal values

APPENDIX A

Table A.1: Statistical droplet sizes results of PEs prepared at 0.6 wt% XG (sample I); 1.4 wt% XG (sample II); 1.6 wt% XG (sample III) concentrations.

PE (I, II, III)	Sum of Squares	df	Mean Square	F	Sig.
Between Groups	163,423	2	81,712	36,347	,000
Within Groups	20,233	9	2,248		
Total	183,656	11			

Table A.2: Multiple comparisons of PEs droplet sizes.

					95% Confidence Interval	
(I) PE	(J) PE	Mean Difference (I-J)	Std. Error	Sig.	Lower Bound	Upper Bound
I	II	-7,98437*	1,06021	,000	-10,9445	-5,0242
	III	-7,66247*	1,06021	,000	-10,6226	-4,7023
II	I	7,98437*	1,06021	,000	5,0242	10,9445
	III	,32190	1,06021	,951	-2,6382	3,2820
III	I	7,66247*	1,06021	,000	4,7023	10,6226
	II	-,32190	1,06021	,951	-3,2820	2,6382

*. The mean difference is significant at the 0.05 level.

APPENDIX B

Table B.1: Statistical hardness results of DEs prepared at 30 wt% SFO (sample IV); 38.3 wt% SFO (sample V); 46.7 wt% SFO (sample VI); 55 wt% SFO (sample VII) concentrations.

DE (IV, V, VI, VII)	Sum of Squares	Df	Mean Square	F	Sig.
Between Groups	205,352	3	68,451	33,238	,000
Within Groups	24,713	12	2,059		
Total	230,066	15			

Table B.2: Multiple comparisons of DEs hardness prepared at 30 wt% SFO (sample IV); 38.3 wt% SFO (sample V); 46.7 wt% SFO (sample VI); 55 wt% SFO (sample VII) concentrations.

					95% Confidence Interval	
(I) DE	(J) DE	Mean Difference (I-J)	Std. Error	Sig.	Lower Bound	Upper Bound
IV	V	3,70487*	1,01475	,015	,6922	6,7176
	VI	5,28734*	1,01475	,001	2,2747	8,3000
	VII	9,98400*	1,01475	,000	6,9713	12,9967
V	IV	-3,70487*	1,01475	,015	-6,7176	-,6922
	VI	1,58248	1,01475	,435	-1,4302	4,5952
	VIII	6,27913*	1,01475	,000	3,2664	9,2918
VI	IV	-5,28734*	1,01475	,001	-8,3000	-2,2747
	V	-1,58248	1,01475	,435	-4,5952	1,4302
	VII	4,69665*	1,01475	,003	1,6840	7,7093
VII	IV	-9,98400*	1,01475	,000	-12,9967	-6,9713
	V	-6,27913*	1,01475	,000	-9,2918	-3,2664
	VI	-4,69665*	1,01475	,003	-7,7093	-1,6840

*. The mean difference is significant at the 0.05 level.

Table B.3: Statistical hardness results of DEs prepared at 30 wt% water (sample VIII); 40 wt% water (sample IX); 45 wt% water (sample X); 60 wt% water (sample XI) concentrations.

DE (VIII, IX, X, XI)	Sum of Squares	df	Mean Square	F	Sig.
Between Groups	5818,753	3	1939,584	117,092	,000
Within Groups	198,776	12	16,565		
Total	6017,528	15			

Table B.4: Multiple comparisons of DEs hardness prepared at 30 wt% water (sample VIII); 40 wt% water (sample IX); 45 wt% water (sample X); 60 wt% water (sample XI) concentrations.

					95% Confidence Interval	
(I) DE	(J) DE	Mean Difference (I-J)	Std. Error	Sig.	Lower Bound	Upper Bound
VIII	IX	31,52645*	2,87790	,000	22,9822	40,0707
	X	19,95228*	2,87790	,000	11,4081	28,4965
	XI	52,67541*	2,87790	,000	44,1312	61,2196
IX	VIII	-31,52645*	2,87790	,000	-40,0707	-22,9822
	X	-11,57417*	2,87790	,008	-20,1184	-3,0300
	XII	21,14896*	2,87790	,000	12,6048	29,6932
X	VIII	-19,95228*	2,87790	,000	-28,4965	-11,4081
	IX	11,57417*	2,87790	,008	3,0300	20,1184
	XII	32,72313*	2,87790	,000	24,1789	41,2673
XI	VII	-52,67541*	2,87790	,000	-61,2196	-44,1312
	IX	-21,14896*	2,87790	,000	-29,6932	-12,6048
	X	-32,72313*	2,87790	,000	-41,2673	-24,1789

*. The mean difference is significant at the 0.05 level.

Table B.5: Statistical hardness results of DEs prepared at 20 wt% water (sample XII) and 26.67 wt% water (sample XIII) concentrations.

DE (XII, XIII)	Sum of Squares	Df	Mean Square	F	Sig.
Between Groups	1,451	1	1,451	,072	,798
Within Groups	121,390	6	20,232		
Total	122,841	7			

APPENDIX C

Table C.1: Statistical T_0, T_p, T_e and ΔH values of DEs prepared at 30 wt% SFO (sample IV); 38.3 wt% SFO (sample V); 46.7 wt% SFO (sample VI); 55 wt% SFO (sample VII) concentrations.

		Sum of Squares	Df	Mean Square	F	Sig.
T_0	Between Groups	15,128	3	5,043	3,314	,139
	Within Groups	6,087	4	1,522		
	Total	21,215	7			
T_p	Between Groups	9,267	3	3,089	4,530	,089
	Within Groups	2,727	4	,682		
	Total	11,994	7			
T_e	Between Groups	1,294	3	,431	8,628	,032
	Within Groups	,200	4	,050		
	Total	1,494	7			
ΔH	Between Groups	29,246	3	9,749	8,468	,033
	Within Groups	4,605	4	1,151		
	Total	33,851	7			

Table C.2: Multiple comparisons T_0 values of DEs prepared at 30 wt% (sample IV); 38.3 wt% (sample V); 46.7 wt% (sample VI); 55 wt% (sample VII) SFO concentrations.

					95% Confidence Interval	
(I) DE	(J) DE	Mean Difference (I-J)	Std. Error	Sig.	Lower Bound	Upper Bound
IV	V	-3,00500	1,23358	,211	-8,0267	2,0167
	VI	-2,36500	1,23358	,349	-7,3867	2,6567
	VII	-3,63500	1,23358	,131	-8,6567	1,3867
V	IV	3,00500	1,23358	,211	-2,0167	8,0267
	VI	,64000	1,23358	,950	-4,3817	5,6617
	VIII	-,63000	1,23358	,952	-5,6517	4,3917
VI	IV	2,36500	1,23358	,349	-2,6567	7,3867
	V	-,64000	1,23358	,950	-5,6617	4,3817
	VII	-1,27000	1,23358	,744	-6,2917	3,7517
VII	IV	3,63500	1,23358	,131	-1,3867	8,6567
	V	,63000	1,23358	,952	-4,3917	5,6517
	VI	1,27000	1,23358	,744	-3,7517	6,2917

Table C.3: Multiple comparisons T_p values of DEs prepared at 30 wt% (sample IV); 38.3 wt% (sample V); 46.7 wt% (sample VI); 55 wt% (sample VII) SFO concentrations.

					95% Confidence Interval	
(I) DE	(J) DE	Mean Difference (I-J)	Std. Error	Sig.	Lower Bound	Upper Bound
IV	V	-2,26500	,82573	,158	-5,6264	1,0964
	VI	-2,63500	,82573	,105	-5,9964	,7264
	VII	-2,50000	,82573	,121	-5,8614	,8614
V	IV	2,26500	,82573	,158	-1,0964	5,6264
	VI	-,37000	,82573	,967	-3,7314	2,9914
	VIII	-,23500	,82573	,991	-3,5964	3,1264
VI	IV	2,63500	,82573	,105	-,7264	5,9964
	V	,37000	,82573	,967	-2,9914	3,7314
	VII	,13500	,82573	,998	-3,2264	3,4964
VII	IV	2,50000	,82573	,121	-,8614	5,8614
	V	,23500	,82573	,991	-3,1264	3,5964
	VI	-,13500	,82573	,998	-3,4964	3,2264

Table C.4: Multiple comparisons T_e values of DEs prepared at 30 wt% (sample IV); 38.3 wt% (sample V); 46.7 wt% (sample VI); 55 wt% (sample VII) SFO concentrations.

					95% Confidence Interval	
(I) DE	(J) DE	Mean Difference (I-J)	Std. Error	Sig.	Lower Bound	Upper Bound
IV	V	-,98000*	,22358	,039	-1,8902	-,0698
	VI	-,74000	,22358	,094	-1,6502	,1702
	VII	-,16500	,22358	,878	-1,0752	,7452
V	IV	,98000*	,22358	,039	,0698	1,8902
	VI	,24000	,22358	,722	-,6702	1,1502
	VIII	,81500	,22358	,071	-,0952	1,7252
VI	IV	,74000	,22358	,094	-,1702	1,6502
	V	-,24000	,22358	,722	-1,1502	,6702
	VII	,57500	,22358	,186	-,3352	1,4852
VII	IV	,16500	,22358	,878	-,7452	1,0752
	V	-,81500	,22358	,071	-1,7252	,0952
	VI	-,57500	,22358	,186	-1,4852	,3352

*. The mean difference is significant at the 0.05 level.

Table C.5: Multiple comparisons ΔH values of DEs prepared at 30 wt% (sample IV); 38.3 wt% (sample V); 46.7 wt% (sample VI); 55 wt% (sample VII) SFO concentrations.

(I) DE	(J) DE	Mean Difference (I-J)	Std. Error	Sig.	95% Confidence Interval Lower Bound	Upper Bound
IV	V	3,55000	1,07293	,094	-,8178	7,9178
	VI	3,53500	1,07293	,096	-,8328	7,9028
	VII	5,25000*	1,07293	,027	,8822	9,6178
V	IV	-3,55000	1,07293	,094	-7,9178	,8178
	VI	-,01500	1,07293	1,000	-4,3828	4,3528
	VIII	1,70000	1,07293	,476	-2,6678	6,0678
VI	IV	-3,53500	1,07293	,096	-7,9028	,8328
	V	,01500	1,07293	1,000	-4,3528	4,3828
	VII	1,71500	1,07293	,470	-2,6528	6,0828
VII	IV	-5,25000*	1,07293	,027	-9,6178	-,8822
	V	-1,70000	1,07293	,476	-6,0678	2,6678
	VI	-1,71500	1,07293	,470	-6,0828	2,6528

*. The mean difference is significant at the 0.05 level.

Table C.6: Statistical T_0, T_p, T_e and ΔH values of DEs prepared at 30 wt% water (sample VIII); 40 wt% water (sample IX); 45 wt% water (sample X); 60 wt% water (sample XI) concentrations.

		Sum of Squares	df	Mean Square	F	Sig.
T_0	Between Groups	51,581	3	17,194	5,247	,072
	Within Groups	13,108	4	3,277		
	Total	64,689	7			
T_p	Between Groups	25,117	3	8,372	13,128	,015
	Within Groups	2,551	4	,638		
	Total	27,668	7			
T_e	Between Groups	5,533	3	1,844	15,517	,011
	Within Groups	,475	4	,119		
	Total	6,009	7			
ΔH	Between Groups	472,570	3	157,523	56,658	,001
	Within Groups	11,121	4	2,780		
	Total	483,691	7			

Table C.7: Multiple comparisons T_0 values of DEs prepared at 30 wt% water (sample VIII); 40 wt% water (sample IX); 45 wt% water (sample X); 60 wt% water (sample XI) concentrations.

					95% Confidence Interval	
(I) DE	(J) DE	Mean Difference (I-J)	Std. Error	Sig.	Lower Bound	Upper Bound
VIII	IX	-6,55000	1,81025	,072	-13,9192	,8192
	X	-4,69500	1,81025	,182	-12,0642	2,6742
	XI	-1,75000	1,81025	,775	-9,1192	5,6192
IX	VIII	6,55000	1,81025	,072	-,8192	13,9192
	X	1,85500	1,81025	,746	-5,5142	9,2242
	XII	4,80000	1,81025	,172	-2,5692	12,1692
X	VIII	4,69500	1,81025	,182	-2,6742	12,0642
	IX	-1,85500	1,81025	,746	-9,2242	5,5142
	XII	2,94500	1,81025	,458	-4,4242	10,3142
XI	VII	1,75000	1,81025	,775	-5,6192	9,1192
	IX	-4,80000	1,81025	,172	-12,1692	2,5692
	X	-2,94500	1,81025	,458	-10,3142	4,4242

Table C.8: Multiple comparisons T_p values of DEs prepared at 30 wt% water (sample VIII); 40 wt% water (sample IX); 45 wt% water (sample X); 60 wt% water (sample XI) concentrations.

					95% Confidence Interval	
(I) DE	(J) DE	Mean Difference (I-J)	Std. Error	Sig.	Lower Bound	Upper Bound
VIII	IX	-4,59000*	,79859	,015	-7,8410	-1,3390
	X	-3,84000*	,79859	,029	-7,0910	-,5890
	XI	-2,05000	,79859	,186	-5,3010	1,2010
IX	VIII	4,59000*	,79859	,015	1,3390	7,8410
	X	,75000	,79859	,788	-2,5010	4,0010
	XII	2,54000	,79859	,106	-,7110	5,7910
X	VIII	3,84000*	,79859	,029	,5890	7,0910
	IX	-,75000	,79859	,788	-4,0010	2,5010
	XII	1,79000	,79859	,255	-1,4610	5,0410
XI	VII	2,05000	,79859	,186	-1,2010	5,3010
	IX	-2,54000	,79859	,106	-5,7910	,7110
	X	-1,79000	,79859	,255	-5,0410	1,4610

*. The mean difference is significant at the 0.05 level.

Table C.9: Multiple comparisons T_e values of DEs prepared at 30 wt% water (sample VIII); 40 wt% water (sample IX); 45 wt% water (sample X); 60 wt% water (sample XI) concentrations.

					95% Confidence Interval	
(I) DE	(J) DE	Mean Difference (I-J)	Std. Error	Sig.	Lower Bound	Upper Bound
VIII	IX	-,65500	,34476	,354	-2,0585	,7485
	X	,60500	,34476	,407	-,7985	2,0085
	XI	1,60500*	,34476	,032	,2015	3,0085
IX	VIII	,65500	,34476	,354	-,7485	2,0585
	X	1,26000	,34476	,070	-,1435	2,6635
	XII	2,26000*	,34476	,010	,8565	3,6635
X	VIII	-,60500	,34476	,407	-2,0085	,7985
	IX	-1,26000	,34476	,070	-2,6635	,1435
	XII	1,00000	,34476	,136	-,4035	2,4035
XI	VII	-1,60500*	,34476	,032	-3,0085	-,2015
	IX	-2,26000*	,34476	,010	-3,6635	-,8565
	X	-1,00000	,34476	,136	-2,4035	,4035

*. The mean difference is significant at the 0.05 level.

Table C.10: Multiple comparisons ΔH values of DEs prepared at 30 wt% water (sample VIII); 40 wt% water (sample IX); 45 wt% water (sample X); 60 wt% water (sample XI) concentrations.

					95% Confidence Interval	
(I) DE	(J) DE	Mean Difference (I-J)	Std. Error	Sig.	Lower Bound	Upper Bound
VIII	IX	17,33500*	1,66740	,002	10,5473	24,1227
	X	17,13500*	1,66740	,002	10,3473	23,9227
	XI	18,63000*	1,66740	,001	11,8423	25,4177
IX	VIII	-17,33500*	1,66740	,002	-24,1227	-10,5473
	X	-,20000	1,66740	,999	-6,9877	6,5877
	XII	1,29500	1,66740	,862	-5,4927	8,0827
X	VIII	-17,13500*	1,66740	,002	-23,9227	-10,3473
	IX	,20000	1,66740	,999	-6,5877	6,9877
	XII	1,49500	1,66740	,808	-5,2927	8,2827
XI	VII	-18,63000*	1,66740	,001	-25,4177	-11,8423
	IX	-1,29500	1,66740	,862	-8,0827	5,4927
	X	-1,49500	1,66740	,808	-8,2827	5,2927

*. The mean difference is significant at the 0.05 level.

Table C.11: Statistical $T_{0,}$ T_p, T_e and ΔH values of DEs prepared at 20 wt% water (sample XII) and 26.67 wt% water (sample XIII) concentrations.

		Sum of Squares	df	Mean Square	F	Sig.
T_0	Between Groups	11,765	1	11,765	11,183	,079
	Within Groups	2,104	2	1,052		
	Total	13,869	3			
T_p	Between Groups	3,010	1	3,010	,804	,465
	Within Groups	7,492	2	3,746		
	Total	10,502	3			
T_e	Between Groups	,245	1	,245	5,695	,140
	Within Groups	,086	2	,043		
	Total	,331	3			
ΔH	Between Groups	59,668	1	59,668	5,910	,136
	Within Groups	20,191	2	10,095		
	Total	79,859	3			

CURRICULUM VITAE

Name Surname **:** Turgay ÇETİNKAYA

Place and Date of Birth **:** Fatih/17.05.1991

E-Mail **:** cetinkayat@itu.edu.tr

EDUCATION:

- **B.Sc.** **:** 2009-2014, Sakarya University, Faculty of Food Engineering, Food Engineering.

PUBLISHED RESEARCH:

- Cetinkaya T, Altay F, "Effects of nanofillers on plant protein based nanocomposites for food packaging applications", 6th INTERNATIONAL SEMINAR ON MODERN POLYMERIC MATERIALS FOR ENVIRONMENTAL APPLICATIONS, Kraków, POLAND, 27-29/04/2016.